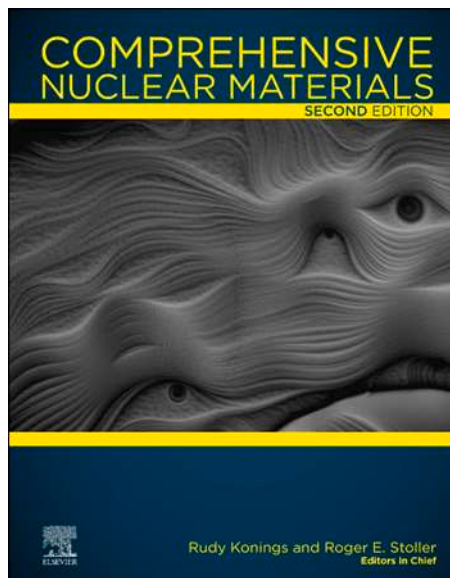


**Provided for non-commercial research and educational use.  
Not for reproduction, distribution or commercial use.**

This article was originally published in *Comprehensive Nuclear Materials*, 2<sup>nd</sup> edition published by Elsevier, and the attached copy is provided by Elsevier for the author's benefit and for the benefit of the author's institution, for non-commercial research and educational use, including without limitation, use in instruction at your institution, sending it to specific colleagues who you know, and providing a copy to your institution's administrator.



All other uses, reproduction and distribution, including without limitation, commercial reprints, selling or licensing copies or access, or posting on open internet sites, your personal or institution's website or repository, are prohibited. For exceptions, permission may be sought for such use through Elsevier's permissions site at:

<https://www.elsevier.com/about/policies/copyright/permissions>

Becquart Charlotte S., Mousseau Normand and Domain Christophe (2020). Kinetic Monte Carlo Simulations of Irradiation Effects. In: Konings, Rudy JM and Stoller Roger E (eds.) *Comprehensive Nuclear Materials 2<sup>nd</sup> edition*, vol. 1, pp. 754–778. Oxford: Elsevier.

<http://dx.doi.org/10.1016/B978-0-12-803581-8.11685-6>

© 2020 Elsevier Ltd All rights reserved.

## 1.24 Kinetic Monte Carlo Simulations of Irradiation Effects<sup>☆</sup>

**Charlotte S Becquart**, University of Lille, CNRS, INRAE, Centrale Lille, UMR 8207 – UMET – Unité Matériaux et Transformations, F-59000, Lille, France

**Normand Mousseau**, Department of Physics and RQMP, Université de Montréal, Montreal, QC, Canada

**Christophe Domain**, EDF-R&D, Department of Materials and Mechanical Components, Les Renardières, Moret sur Loing Cedex, France

© 2020 Elsevier Ltd. All rights reserved.

<b>1.24.1</b>	<b>Introduction</b>	754
<b>1.24.2</b>	<b>Method</b>	755
1.24.2.1	Classical Approach: Predetermined Event List	757
1.24.2.2	On-the Fly KMCs	757
<b>1.24.3</b>	<b>Radiation Damage Specific Issues</b>	759
1.24.3.1	Irradiation (Introduction of Cascades, FP)	759
1.24.3.2	Point Defect Fluxes	760
1.24.3.3	Formation and Migration of SIAs and SIA Clusters/Loops	760
1.24.3.4	Ballistic Mixing	760
1.24.3.5	Transmutation	761
<b>1.24.4</b>	<b>KMC Studies Related to Radiation Damage</b>	761
1.24.4.1	Annealing of Cascades and Source Term Determination	761
1.24.4.2	Precipitation, Segregation and Phase Transformations	761
1.24.4.3	Typical Damage Accumulation/Microstructure Evolution: Impact of Dose, Temperature, Impurities ...	765
1.24.4.4	Solute or Impurity/Gas Atoms Diffusion and the Formation of Gas Bubbles	766
1.24.4.5	Investigating Solutions to Eliminate the Point Defects or Trap Gas Atoms	769
<b>1.24.5</b>	<b>Comparison of Models</b>	770
<b>1.24.6</b>	<b>Coupling With Other Methods</b>	770
<b>1.24.7</b>	<b>Locks/Things That Need to be Investigated/Improved Further</b>	770
<b>1.24.8</b>	<b>Conclusions</b>	772
<b>References</b>		772

### Abbreviations

AKMC Atomic Kinetic Monte Carlo  
 BKL Bortz, Kalos, Lebowitz algorithm  
 DFT Density Functional theory  
 dpa Displacement per atom  
 EKMC Event Kinetic Monte Carlo  
 ER Electrical resistivity  
 FP Frenkel pair  
 GB Grain boundaries  
 KMC Kinetic Monte Carlo

MC Monte Carlo  
 MD Molecular dynamics  
 MFRT Mean field rate theory  
 OKMC Object Kinetic Monte Carlo  
 PKA Primary knocked-on atom  
 RIS Radiation induced segregation  
 RTA Residence time algorithm  
 SIA Self interstitial atom  
 TST Transition state theory

### 1.24.1 Introduction

Along with molecular dynamics (MD), Monte Carlo (MC) methods are among the most used techniques for modeling materials at the atomic scale. The name MC comes from the fact that this method, derived from statistical physics, uses random numbers similar to those involved in the game of roulette. The techniques of MC were initially used in the US Manhattan project in the 1940s and saw further development in the later project to develop the hydrogen bomb. At that time, it was possible to simulate only a few hundred atoms.<sup>1</sup> Today simulations of several million atoms and several billion steps are quite common. Two main types of algorithms have been generated. The classic algorithm of MC developed by

<sup>☆</sup>*Change History:* May 2019. Charlotte S. Becquart, Normand Mousseau and Christophe Domain have updated the figures, text and references.

This is an update of Becquart, C.S., Wirth, B.D., 2012. Chapter 1.14 – Kinetic Monte Carlo Simulations of Irradiation Effects. In: Konings, R.J.M. (Ed.), Comprehensive Nuclear Materials, Elsevier, pp. 393–410.

Metropolis<sup>2</sup> focuses on sampling a given configuration space in order to construct statistical ensemble properties of the system. Focusing on equilibrium, Metropolis MC allows the use of a rich variety of moves and importance sampling distributions to sample complex landscape, with the caveat that time is not directly accessible in the standard approach. The Kinetic Monte Carlo family of algorithms removes this problem when the microscopic mechanism(s) leading to a change of configuration are known. In this case, time can be introduced, at the cost, of course, of limiting the sampling efficiency. The latter method is, however, essential to deal with problems of diffusion and transport in solids and is the topic of this article.

### 1.24.2 Method

The Monte Carlo method was originally developed by von Neumann, Ulam and Metropolis to study the diffusion of neutrons in fissionable material on the Manhattan Project and first applied to simulating radiation damage of metals more than 50 years ago by Besco,<sup>3</sup> Doran<sup>4</sup> and later Heinisch and co-workers.<sup>5</sup>

Monte Carlo is a stochastic process and utilizes random numbers to select event probabilities from probability distributions and generate atomic configurations,<sup>6</sup> rather than the deterministic manner of molecular dynamics simulations, but remains as statistically exact, and often more efficient, when computing ensemble, or in the case of KMC methods, dynamic properties. While different Monte Carlo applications are used in computational materials science, we shall focus our attention on Kinetic Monte Carlo (KMC) simulation as applied to the study of radiation damage.

The KMC methods used in radiation damage studies represent a subset of MC methods that can be classified as rejection-free, in contrast with the more classical MC methods based on the Metropolis algorithm<sup>2,7</sup>. They provide a solution to the Master Equation which describes a physical system whose evolution is governed by a known set of transition rates between possible states.<sup>8</sup> The solution proceeds by choosing randomly among the various possible transitions and accepting them on the basis of probabilities determined from the corresponding transition rates. These probabilities are calculated for physical transition mechanisms as Boltzmann factor frequencies, and the events take place according to their probabilities leading to an evolution of the microstructure. The main ingredients of such models are thus a set of objects (which can resolve to the atomic scale as atoms, or point defects) and a set of reactions or (rules) that describe the manner in which these objects undergo processes such as diffusion, emission, other reactions, and their rates of occurrence.

Many of the KMC techniques are based on the residence time algorithm (RTA) derived fifty years ago by Young and Elcock<sup>9</sup> to model vacancy diffusion in ordered alloys. Its basic recipe involves the following: for a system in a given state, instead of making a number of unsuccessful attempts to perform a transition to reach another state, as in the case of the Metropolis algorithm,<sup>2,7</sup> the average time the system remains in a given state is calculated. A transition to a different state is then performed based on the relative weights determined amongst all possible transitions, which also determines the time increment associated with the selected transition. According to standard transition state theory (see for instance 10) the frequency  $\Gamma_x$  of a thermally activated event  $x$ , such as a vacancy jump in an alloy or the jump of a vacancy cluster can be expressed as:

$$\Gamma_x = \nu_x \exp\left(-\frac{E_a}{k_B T}\right) \quad (1)$$

where  $\nu_x$  is the attempt frequency,  $k_B$  is Boltzmann's constant,  $T$  is the absolute temperature and  $E_a$  is the activation energy of the jump.

During the course of a KMC simulation, the probabilities, here assimilated to the transition frequencies  $\Gamma_x$ , of all possible transitions are calculated and one event is chosen at each time-step, by extracting a random number  $\xi$ , and comparing it to the relative probability as illustrated in Fig. 1. The associated time-step length,  $\delta t$ , and average time-step

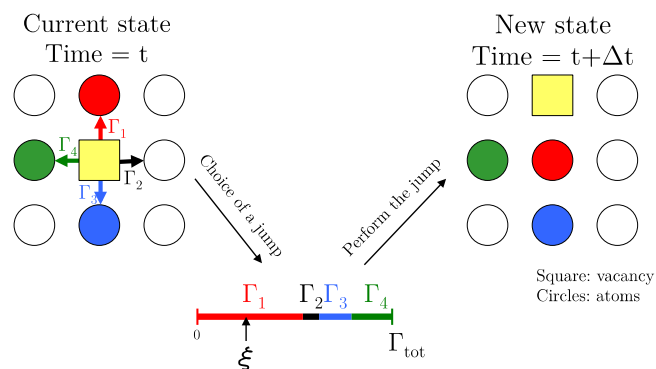


**Fig. 1** Representation of the KMC algorithm on a 2D square lattice with one vacancy performing a transition with one of its first nearest neighbors.  $\xi$  is the random number, usually chosen between 0 and 1 because the sum of the probabilities  $\Gamma_{tot}$ , is usually normalized to one.

length,  $\Delta t$ , are given by:

$$\delta t = \frac{-\ln r}{\sum_x \Gamma_x} \quad (2)$$

$$\Delta t = \frac{1}{\sum_x \Gamma_x} \quad (3)$$

where  $r$  is a random number between 0 and 1. The residence time algorithm is also known as the BKL (Bortz, Kalos, Lebowitz) algorithm.<sup>11</sup> Other techniques are possible, as described by Chatterjee and Vlachos.<sup>12</sup>

The basic steps in a KMC simulation can thus be summarized as:

- (1) Calculate the probability (rate) for a given event to occur.
- (2) Sum the probabilities of all events to obtain a cumulative distribution function.
- (3) Generate a random number to select an event from all possible events.
- (4) Increment the simulation time based on the inverse sum of the rates of all possible events (Eq. (2)).
- (5) Perform the selected event and all spontaneous events as a result of the event performed.
- (6) Repeat steps 1 through 4 until the desired simulation condition is reached.

Kinetic Monte Carlo models are now widely used for simulating radiation effects on materials as we will demonstrate in this article. Advantages of KMC models include the ability to capture spatial correlations in a full three-dimensional simulation with atomic resolution, while ignoring the atomic vibration time scales captured by molecular dynamics models, as well as the possibility to work on multiple scales. Indeed, with KMC, individual point defects, point defect clusters, solutes and impurities can be treated as objects, either on or off an underlying crystallographic lattice, as the evolution of these objects is modeled over time. Two general approaches have been used in KMC simulations, event KMC<sup>13–15</sup> and object KMC. These two differ in the treatment of time scales or step between individual events. Within the object KMC designation, it is also possible to further sub-divide the techniques into those that explicitly treat atoms and atomic interactions, which is often denoted as atomic Kinetic Monte Carlo (AKMC), or Lattice KMC (LKMC), and which was reviewed by Becquart and Domain,<sup>16</sup> versus those that track the defects on a lattice, but without complete resolution of the atomic arrangement. This later technique is predominately referred to as object Monte Carlo (OKMC), and used in such codes as BigMac,<sup>17,18</sup> LAKIMOCA,<sup>19</sup> MMonca<sup>20</sup> and others. In this article, we will designate by OKMC, the mesoscopic version of the object kinetic MC and by AKMC the atomistic version of the object kinetic MC; their respective frameworks are illustrated in Fig. 2. AKMC simulations are more precise but, as a consequence, are more time consuming. The basic problem is, for this approach, to give a realistic description of all the relevant atomic displacement mechanisms: the displacements directly resulting from radiation damage, ballistic mixing as well as the thermally activated jumps of point defects, the point defect elimination mechanisms,

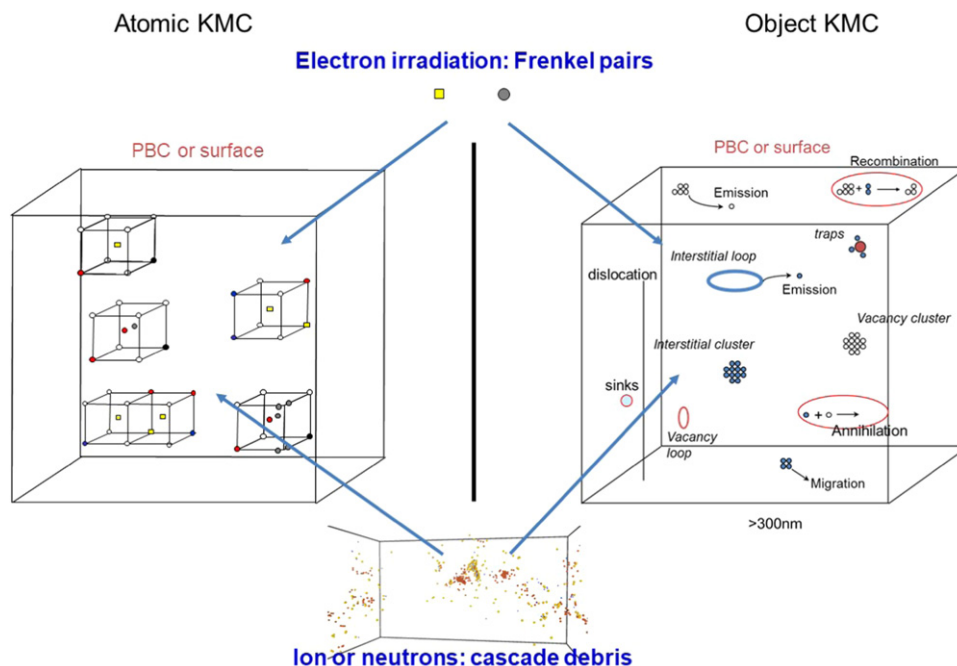


**Fig. 2** AKMC supercell (left) vs. OKMC supercell (right). The AKMC considers atoms and point defects whereas the OKMC considers objects. In the AKMC a 5 vacancy cluster is made of 5 vacancies that behave independently from one another, whereas in the OKMC a 5 vacancy cluster is a single object. In both approaches, the irradiation consists in the introduction of point defects, isolated or in clusters depending on the irradiation type. Reproduced from Stoller, R., 2020. Primary Radiation Damage Formation, Comprehensive Nuclear Materials, second ed. pp. 620–662.

including the way the point defect or solute migration barriers depend on the local atomic environment. In OKMC (the object version of it) and EKMC simulations, the challenge is to determine the relevant mechanisms that can be activated as well as the necessary effective parameters, which are usually obtained from atomic models.

As KMC modeling of radiation damage involves tracking the location and fate of all defects, impurities and solutes as a function of time to predict microstructural evolution, the starting point in these simulations is often the primary damage state, i.e., the spatially correlated locations of vacancies, self-interstitials and transmutants produced in displacement cascades<sup>21,22</sup> resulting from irradiation and obtained from MD<sup>23,24</sup> or the binary collision approximation (BCA)<sup>25</sup> simulations, along with the displacement or damage rate which sets the time scale for defect introduction. The rates of all reaction – diffusion events then control the subsequent evolution or progression in time, and are determined from appropriate activation energies for diffusion, dissociation, and other reactions that occur between species. These energies are key input parameters, which, as stated previously, are assumed to be known. The defects execute random diffusion jumps (in one, two or three dimensions depending on the nature of the defect) with a probability (rate) proportional to their diffusivity. Similarly, cluster dissociation rates are governed by a dissociation probability that is controlled by the binding energy of a particle to the cluster. The events to be performed and associated time step for each Monte Carlo sweep are chosen from the RTA.<sup>9,11</sup> The list of possible events can be either predetermined or calculated on-the-fly as will be discussed in the next section. Note that in the EKMC approach,<sup>13–15</sup> the microstructure also consists of objects. The crystal lattice is ignored and objects' coordinates can change continuously. The only events considered are those which lead to a change in the defect population, namely: clustering of objects, emission of mobile species, elimination of objects on fixed sinks (surface, dislocation), or the annihilation of objects on their anti-defect. The migration of an object in its own right is considered an event only if it ends up with a reaction which changes the defect population. In this case the migration step and the reaction are processed as a single event; otherwise, the migration is performed only once at the end of the EKMC time interval  $\Delta t$ . In contrast to the residence time algorithm, where all rates are lumped into one total rate to obtain the time increment, in an EKMC scheme the time delays of all possible events are calculated separately and sorted by increasing time increment in a list. The event corresponding to the shortest delay,  $\tau_s$ , is processed first, and the remaining list of delay times for other events is modified accordingly by eliminating the delay time associated with the particle that just disappeared, adding delay times for a new mobile object, etc. A comparison between EKMC and OKMC can be found in Refs. 26,27.

#### 1.24.2.1 Classical Approach: Predetermined Event List

The traditional approach to KMC has been to build a list of predetermined events with their associated activation energy. For the diffusion events, the activation energies are the migration energies (and jump frequencies) of the moving species: point defects, point defect clusters, transmutants or solute atoms as well as Foreign Interstitial Atoms (FIA) such as carbon, helium and hydrogen, isolated or in clusters with or without point defects. When the local chemical environment is complex, i.e., when the system is composed of several atomic elements, these data are not straightforward to evaluate and often associated with this approach has been the use of rigid lattices. The rigid lattice approximation allows a fast estimation of the activation barriers through simple heuristic approaches such as the kinetically resolved activation (KRA), according to Van der Ven,<sup>28</sup> or final initial state energy (FISE) approximation, according to the terminology adopted by Vincent *et al.*<sup>29</sup> based on the Kang and Weinberg decomposition of migration energy barriers.<sup>30</sup> Such simple models include broken bonds or cut bond models<sup>31</sup> as well as models based on cluster expansions of the Hamiltonian,<sup>32</sup> the simplest ones being pair models.<sup>33–35</sup> When interatomic potentials are available for the material modeled, then clever techniques such as artificial neural network (ANN)<sup>36–38</sup> can also be used. Interatomic potentials have limitations, however, and are only available at the moment, often with limited precision, for simple materials such as binary or ternary alloys.<sup>39</sup> Nevertheless, interatomic potentials are often essential since they permit the elimination of the rigid lattice constraint as the activation barriers can be determined no matter the positions of the atoms around the moving species.

#### 1.24.2.2 On-the Fly KMCs

Restriction to lattice positions greatly limits the applications of KMC when evolving the system, but is imposed for technical reasons. Diffusion mechanisms can become rapidly complex and difficult to predict in distorted and irregular environments. They are, moreover, generally difficult to classify, especially before the launch of a simulation, which greatly limits the capacity to construct a relevant event catalog.

Overcoming these limitations is challenging and computationally costly. The first off-lattice KMC simulation was performed by Henkelman and Jónsson<sup>40</sup> looking at Al on Al growth. Without a catalog, the simulation generated an event list at every step, using 25 open-ended saddle searches generated with the dimer method. While the number of searches was too small to ensure that all events had been found, this work still identified new extended low-barrier events that modified considerably the kinetics of growth. Over the following years, a number of approaches were introduced to reduce the computational cost of off-lattice KMC simulations by introducing a cataloging approach. While still lattice-based, Trushin *et al.*<sup>41</sup> introduced an algorithm where the catalog was adjusted on-the-fly as the system evolved, allowing the study of more complex environments and, more important, the inclusion, in the barrier calculation, of a larger area, going beyond the standard first and second neighbor shells.

The first off-lattice KMC algorithm with on-the-fly cataloging was introduced by El-Mellouhi *et al.*<sup>42</sup> Coupling an open-search method, the activation-relaxation technique (ART nouveau)<sup>43,44</sup> with a topological classification, NAUTY,<sup>45,46</sup> the kinetic

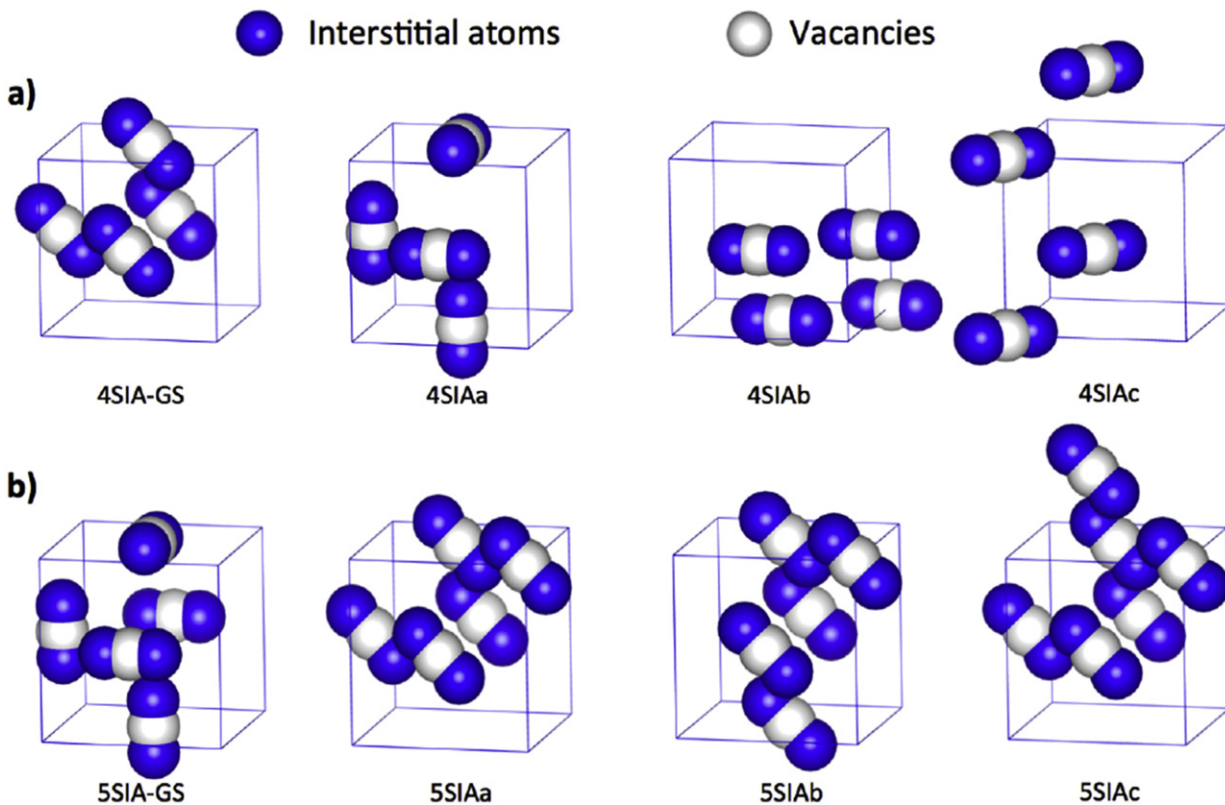


**Fig. 3** Schematic illustration of lowest-energy states for one to five self-defects in nickel using an EAM potential, these ground states were generated through KMC evolution using k-ART, allowing to take into account full elastic deformations. Starting from a random distribution of interstitials, the kinetic evolution of each 4000+ interstitial atoms system is allowed to proceed, unbiased, at 500K. (1) Ground states for vacancies and (2) self-interstitials. (a), (b), (c), (d) and (e) present the structure with one, two, three, four and five mono-self-defects for each case. From Mahmoud, S, Trochet, M, Restrepo, O.A., Mousseau, N., 2018. Study of point defects diffusion in nickel using kinetic activation-relaxation technique. *Acta Mater.* 144, 679–690. doi:10.1016/j.actamat.2017.11.021.

activation-relaxation technique (k-ART) associates local graphs with a unique event list, that is generated as new topologies are identified. By removing the need for an underlying crystalline lattice, k-ART allows the creation of event catalogs for any environment even fully disordered.<sup>47–49</sup> These generic cataloged events provide the basis for computing the specific energy barrier associated with each relevant event, as its exact geometry is reconstructed and exactly converged to the real saddle point. Such effort is costly, of course, even with the creation of an event catalog that reduces significantly the time spent for searching for events. This additional expense is well worth it in many cases, even for apparently simple systems as demonstrated by the unexpectedly rich event catalog generated by k-ART for point defects (vacancies and interstitials) in crystalline Fe.<sup>50</sup> Vacancy diffusion and clustering processes in body-centered-cubic (bcc) Fe were studied using the kinetic activation-relaxation technique (k-ART), an off-lattice Kinetic Monte Carlo method with on-the-fly catalog building capabilities.<sup>50</sup> For monovacancies and divacancies, k-ART recovered previously published results while clustering in a 50-vacancy simulation box agreed with experimental estimates. Applying k-ART to the study of clustering pathways for systems containing from one to six vacancies, allowed to find a rich set of diffusion mechanisms. In particular, it was shown that the path followed to reach a hexavacancy cluster influences greatly the associated mean-square displacement. Aggregation in a 50-vacancy box also showed a notable dispersion in relaxation time associated with effective barriers varying from 0.84 to 1.1 eV depending on the exact pathway selected. The effects of long-range elastic interactions between defects were isolated by comparing to simulations where those effects were deliberately suppressed. This allowed to demonstrate that in bcc Fe, suppressing long-range interactions mainly influences kinetics in the first 0.3 ms, slowing down quick energy release cascades seen more frequently in full simulations, whereas long-term behavior and final state are not significantly affected.<sup>50</sup> Similar studies were performed in Si<sup>51</sup> and Ni,<sup>52</sup> with the identification of previously unreported multistep diffusion mechanisms that are as fast or even faster than those used generally. For example, while the barrier for the single Ni self interstitial is only 0.15 eV, Ni tetra-self-interstitials (Fig. 3) diffuse with almost zero energy barrier (0.004 eV) through a three-step process involving a rotation and a jump mechanisms.<sup>52</sup>

Off-lattice KMC methods are even more important when strain and randomness play an important role, such as for characterizing the  $\langle 100 \rangle$ -interstitial loop formation in Fe,<sup>53</sup> following the relaxation of ion-bombarded silicon over long-time (more than 1 s)<sup>48</sup> or understanding C diffusion at an Fe grain boundary, where pathways are strongly influenced by the local deformation.<sup>54</sup>

Over the last decade, a number of other off-lattice or near-off lattice approaches have been proposed, with or without a catalog. Xu *et al.*<sup>55</sup> for example, proposed the Self-Evolving Atomistic Kinetic Monte Carlo (SEAKMC), which defines active volume over which activated mechanisms are searched. As discussed recently,<sup>56</sup> while SEAKMC and k-ART produce similar results, the first method is faster in simpler environments, such as the recombination of a Frenkel pair<sup>57</sup> while the second one is more flexible for handling complex materials.

All KMC methods, including those off-lattice, are only as good as their event catalog and their evaluations of the respective rates. While open-ended search algorithms, such as ART nouveau, provide extensive catalogs,<sup>44</sup> none can guarantee completeness. To alleviate this limitation,<sup>58</sup> introduced a coupling with high temperature molecular dynamics to obtain a better evaluation of the error on the catalog. This analysis is valid as long as the harmonic approximation of transition state theory is valid, i.e., as long as attempt frequencies are not affected by the temperature, which is the standard approximation used in KMC approaches. Yet, recent results show that this approximation is not valid when the barrier energy is comparable to the temperature.<sup>59</sup> This suggests that in the presence of a wide barrier distribution: (i) the harmonic approximation does not provide the correct rates and (ii) it is not possible to rely on high-temperature MD to evaluate low-temperature kinetics.

Off-lattice adaptive KMC methods are opening the application of accelerated methods to more complex environments and systems, providing precise and detailed information as to the dynamics of complex materials. At the same time, these applications are forcing a reevaluation of standard approximations, such as the harmonic approximation in transition state theory (TST), and the use of relatively simple force fields in non-crystalline and multicomponent environments. We can expect considerable developments over the coming decade to widen the scope of application of these methods along with new insights over questions that had been long neglected by lack of access to the appropriate time and length scales. At the moment, however, given their cost, compared with lattice-based KMC methods, off-lattice approaches, such as k-ART, are best used for specific problems. First, disordered environments, where no other method can be applied. Second, systems where the possible number of environments is unknown or too large to systematically explore before hand. At the moment, however, while active development is going on regarding this issues and solutions could be introduced in the near future, the handling of complex ensemble of atoms/defects moving together (such as handled in object KMC), large moving defects (e.g., dislocations) and parallel evolution of a number of independent structures is limited.

Note that rigid lattices are not mandatory either for larger scale KMC approaches such as OKMC and EKMC, as demonstrated for instance in the codes BIGMAC<sup>18</sup> and JERK.<sup>15</sup>

On-the-fly off lattice KMC is one of the methods that allow to go beyond the reaches of classical MD along with other long time scale atomic methods such as various accelerated MD methods.<sup>23,60–62</sup> Choosing between these MD methods and off-lattice KMC approaches, which are much heavier, computationally speaking, than lattice-based, is, therefore, not automatic. While each problem is specific and methods evolve rapidly, as a general rule, accelerated MD methods are efficient when the energy distribution of the relevant barriers is narrow and relatively well separated from the other mechanisms in the simulation. Off-lattice KMC are better at handling flickers and treating wider energy barrier distributions.

Now that the basis of the KMC methods have been introduced, we present the specific issues pertinent to the understanding of radiation damage and how they are / can be implemented using KMC techniques.

### 1.24.3 Radiation Damage Specific Issues

The KMC technique has been applied to a large range of materials science phenomena such as film deposition,<sup>63</sup> corrosion,<sup>64,65</sup> precipitation.<sup>66</sup> Each phenomenon needs to be described in its own way and the next section presents the peculiarity of radiation damage modeling. For a description of radiation effects on microstructures see for instance Ref. 67.

#### 1.24.3.1 Irradiation (Introduction of Cascades, FP)

As mentioned in the introduction and Ref. 67, the introduction of high energy particles (neutrons, ions...) will create a damage that depends, among other factors, on the flux of these particles. The "irradiation" rate, i.e., the rate of impinging particles is usually transformed into a production rate (number per unit time and volume) of randomly distributed displacement cascades of different energies (5, 10, 20, ... keV), as well as residual Frenkel Pairs (FP). New cascade debris are then injected randomly in the simulation box, at the corresponding rate. The cascade debris can be obtained by MD simulations for different recoil energies  $T$ , or introduced based on the number of FP expected from displacement damage theory. In the case of KMC simulation of electron irradiation, FPs are introduced randomly in the simulation box according to a certain dose rate, assuming most of the time that each electron is responsible for the formation of only one FP. This assumption is valid for electrons with energies close to 1 MeV (much lower energy electrons may not produce any FP, whereas higher energy ones may produce small displacement cascades with the formation of several vacancies and self interstitial atoms (SIAs)).

The dose is updated by adding the incremental dose associated with the scattering event of recoil energy  $T$ , using the Norgett-Robinson-Torrens expression<sup>68</sup> for the number of displaced atoms.<sup>24</sup> In this model, the accumulated number of displaced atoms is given by:

$$\text{displacements per event} = 0.8T/2E_D$$

where  $T$  is the damage energy, i.e., the fraction of the energy of the particle transmitted to the Primary Knocked-on Atom (PKA)<sup>24</sup> that is dissipated as kinetic energy in subsequent collisions and  $E_D$  is the threshold displacement energy (e.g., 40 eV for Fe and Reactor Pressure Vessels (RPV) steels<sup>69</sup>).

The production rate (the number and energy of the PKAs, i.e., the PKA spectrum) are typically obtained from codes based on the Binary Collision Approximations (BCA) such as SRIM<sup>70</sup> or Marlowe<sup>71</sup> but other approximations and codes are available.<sup>25</sup> In the case of ion implantation, one further needs to know the ion as well as the point defect implantation profiles. Long term simulations of accumulation of cascades have been modeled using KMC techniques.<sup>72-77</sup> There are ways to investigate the sensitivity of the system to the properties of the displacement cascades (their spatial extent, morphology and the spatial correlation of defects) in the evolution of point defect cluster size distributions. It has been shown that there is no simple answer and the sensitivity can be little or strongly dependent on other parameters such as the mobility of defects, the type of interactions, the presence of impurities and the temperature.<sup>74-76</sup> Additional work is thus needed to obtain a more reliable estimate of the primary damage, for the full high energy particle (neutrons, Fe and to a lesser extent electrons) spectra, particularly in alloys.

### 1.24.3.2 Point Defect Fluxes

As mentioned previously, one of the consequences of irradiation is the formation of a large amount of point defects of both types: vacancies and SIAs that will migrate in the material, creating fluxes of point defects which may be accompanied by solute atoms. It was shown in many cases that the interaction between the point defects and solutes can provide the driving force for solute segregation and precipitation when local solubility limits are exceeded. This leads to complex microstructural evolution, which depends on the atomic-scale diffusion properties used in the models.<sup>78</sup> Usually the rates of diffusion can be obtained from the knowledge of the migration barriers. These, or at least the most important, must then be known for all the diffusing "objects"; i.e., for the point defects in AKMC, OKMC and EKMC, or the clusters in OKMC or EKMC. For isolated point defects, the migration barriers can be obtained from experimental data, i.e., from diffusion coefficients, or theoretically, using the different approaches described in Section 1.24.2.1, or directly from either ab initio calculations as described for instance in Refs. 79,80 or MD simulations as described in Ref. 81. Permanent fluxes of point defects towards the sinks are thus sustained by irradiation: the flux of SIAs corresponding to a flux of atoms towards the sinks, whereas the flux of vacancy corresponds to a flux of atoms away from the sinks. These fluxes will lead to microstructural changes such as precipitation or segregation as described in Ref. 66 and in more detail in Ref. 82. It is thus important to model correctly the diffusion properties of the moving species as well as the "trapping" properties of the different sinks: free surfaces, grain boundaries, dislocations... or traps. A typical example is the impact of point defect diffusion on Zr growth as shown in Ref. 83.

### 1.24.3.3 Formation and Migration of SIAs and SIA Clusters/Loops

Irradiation will lead to the disruption of the crystallinity and the formation of numerous point defects which would not be present in such large amounts in the material under equilibrium conditions. This is particularly the case of SIAs which are not found in metals under thermal equilibrium because of their large formation energies (around 4 eV for Fe, 10 eV for W) and their very low migration barriers (around 0.3 eV in Fe, and close to 0 in W). SIAs move very quickly and tend to form clusters in the form of dislocation loops: dislocation loops of interstitial type have been observed in all kinds of irradiated alloys: RPV steels, model alloys (FeCu, FeMnNi, FeCuNiMn), Fe, W and W alloys ...<sup>84-87</sup>. One issue regarding SIA loops is their burgers vector. For instance, in Fe, two kinds of loops are observed:  $\frac{1}{2} \langle 111 \rangle$  loops which move very easily by one dimensional glide<sup>88</sup> specially at low temperatures<sup>89</sup> and  $\langle 100 \rangle$  loops which are sessile. It is thus important to, on the one hand, include in the KMC models the correct amount of each family of loops and, on the other hand, to model correctly their mobility or lack thereof. Indeed, when they are mobile, SIA loops move very quickly in a 1D motion. This has an impact on their sink strength, i.e., their capacity to interact/attract other point defects and solute atoms. This has been demonstrated in various cases using KMC.<sup>90-95</sup> Furthermore, the interaction of these loops with other loops or solute atoms can lead to changes in the loop Burgers vector and thus in their mobility. This has been recently the scope for on-the-fly KMC simulations<sup>53,96</sup> and needs to be accounted for in modeling microstructure evolution under irradiation. Another issue related to the formation and the mobility of SIA loops is that they interact with solute atoms.<sup>97</sup> KMC studies have shown that solute atoms can confine SIA loop diffusion to short segments,<sup>98</sup> slow down the loops as proposed in Ref. 99 and change the loop saturation density.<sup>100</sup> It is thus necessary to implement these effects correctly, either by introducing the solutes explicitly in the simulation as in Refs. 98,100-102 or implicitly by changing the diffusion properties of the loops to reflect the alloying content as in Refs. 99,103. Another complication with SIA clusters and loops is the fact that the strain they generate in the lattice is not negligible and should be accounted for. KMC simulations have indeed shown that the elastic interaction between defects has an impact on point defect recombination and the formation of clusters,<sup>104</sup> the trapping of SIA clusters<sup>90</sup> or that of dislocation loops.<sup>105</sup> Another demonstration of the importance of elastic interactions can be found in Ref. 106. These authors showed that elastic interactions help SIAs rotate and organize themselves into rafts or dislocation decorations. Note that impurities and solute atoms also interact with vacancy clusters and loops<sup>107</sup> but this has not been so far the object of many KMC simulations.<sup>99</sup>

### 1.24.3.4 Ballistic Mixing

Ballistic mixing refers to the athermal (i.e., not depending on temperature) displacements of atoms within displacement cascades. It always tends to disorder the alloys, irrespective of their equilibrium properties and can lead to precipitate or nanoparticle

dissolution.<sup>108–111</sup> It has been proposed for instance as a reason for the lack of  $\alpha'$  precipitation in FeCr alloys irradiated under high ion flux when the concentration of sinks is high enough.<sup>110</sup> Ballistic mixing is thus an irradiation effect competing with the acceleration of diffusion due to the introduction of point defect supersaturations. A ballistic diffusion coefficient can be defined, that depends on the dose and the number of replacement per displacement.<sup>112</sup> KMC simulations have shown that these competing effects can lead to complex microstructures: different stages of order,<sup>113</sup> the roughening of interfaces, self-organization of precipitates at a mesoscale,<sup>114,115</sup> and patterning.<sup>116</sup>

### 1.24.3.5 Transmutation

The rate of producing atomic transmutation products can also be included in KMC models, as determined from the reaction rate density determined from the product of the neutron cross section and neutron flux. Like the irradiation rate, the volumetric production rate is used to introduce an appropriate number of transmutants, such as helium that is produced by  $(n,\alpha)$  reactions in the fusion neutron environment, where the species are introduced at random locations within the material. In W, transmutation will for instance lead to the formation of Re and Os in non-negligible amounts.<sup>117</sup> These elements have a strong impact on the mobility of SIAs<sup>118,119</sup> and can lead to the formation of brittle intermetallic phases.

The next section is devoted to presenting typical studies pertaining to radiation damage undertaken using the KMC approach.

## 1.24.4 KMC Studies Related to Radiation Damage

### 1.24.4.1 Annealing of Cascades and Source Term Determination

A large number of KMC simulations has been dedicated to the investigation of cascade annealing either to study the cascade survival efficiency of defects produced in cascades (i.e., how many point defect survive intracascade recombination and will feed the point defect fluxes) as in Refs. 19,81,120–129 or to produce the source term for other mesoscale codes such as rate equation cluster dynamics.<sup>130–132</sup> These studies have shown that the relative mobilities of point defects and point defect clusters as well as the migration mechanisms (Figs. 4 and 5) have a crucial impact on the cascade efficiency and the annealing of the cascades.<sup>19,125,133,134</sup> Depending on the material, the most mobile defect may be the SIA or the vacancy, and it was shown that both the relative point defect clustering trends versus temperature and the different mobilities of SIAs and vacancies, changes the annealing efficiency i.e., (the ratio of the number of defects after and before annealing). In W, it exhibits an inverse U-shape curve as a function of temperature.<sup>133</sup> In some very specific cases, it is possible to neglect some of the point defect reactions thus speeding up the calculations as was shown by Pelaz *et al.*<sup>121</sup> in ion implanted Si, but in general one must account explicitly for both point defect populations. Furthermore, the very recent study by Jourdan and Crocombette<sup>132</sup> shows that the cascade annealing depends on the point defect concentrations and must thus be evaluated on-the-fly or for different point defect concentrations unlike how it has been typically done.

The main outcome of all these studies is to point out as in the previous section that it is necessary to have a better understanding of how the point defect and point defect clusters mobilities are affected by solutes, temperatures and other point defects.

### 1.24.4.2 Precipitation, Segregation and Phase Transformations

Point defect fluxes in the materials along with ballistic mixing can lead to phase transformations or segregation at extended defects. In the case of phases predicted by thermodynamics, the irradiation will just accelerate the phase transformation in what is referred to as irradiation enhanced phase transformation, a typical example is the formation of Cu precipitates in Fe. In other cases, the irradiation induces the transformation into a non-equilibrium phase, perhaps by changing the solubility limit as has been observed in the FeCr system.<sup>135</sup> kMC, and more precisely AKMC has been used to study phase transformations for more than twenty years first in binary ferritic alloys (FeCu and FeCr), then in more complex ones such as dilute Fe based alloys representative of RPV steels. Austenitic steels are much more complicated to model because they are paramagnetic and in metastable states. Deriving cohesive models of paramagnetic and/or metastable states is much more difficult, which probably explains why, at the moment, not that many KMC studies have been devoted to these alloys even though RIS is frequently observed at grain boundaries. For ferritic alloys, the historic case is the modeling of copper rich precipitates (CRPs) in bcc  $\alpha$ -Fe. Cu is of primary importance in the embrittlement of the neutron-irradiated RPV steels. It has been observed to segregate into copper-rich precipitates within the ferrite matrix under irradiation. Since its role was discovered more than 50 years ago,<sup>136</sup> Cu precipitation in  $\alpha$ -Fe (Fig. 6) has been observed by atom probe tomography, small angle neutron scattering, and high resolution transmission electron microscopy. Numerical simulation techniques such as rate theory or AKMC methods have also been used to investigate this problem<sup>31,137–144</sup>; for a review see Ref. 145. Other solutes present in RPV steels were more recently found to segregate and have been studied. In agreement with experimental observations, the addition of Ni has been found to promote the formation of a higher density of smaller CRPs in binary Fe-Cu alloys, and copper-shell microstructures have been observed in Fe-Cu, Mn, Si.<sup>146,147</sup> Very recently in a study of thermal ageing, it was found that Ni promotes the nucleation of Cu clusters and delays the precipitation kinetics during the coarsening stage because it slows down the Cu clusters<sup>148</sup> that are otherwise more mobile than isolated Cu atoms which migrate by a vacancy mechanism.<sup>149</sup> More complex RPV based alloys have also been investigated,<sup>30,32,150,151</sup>

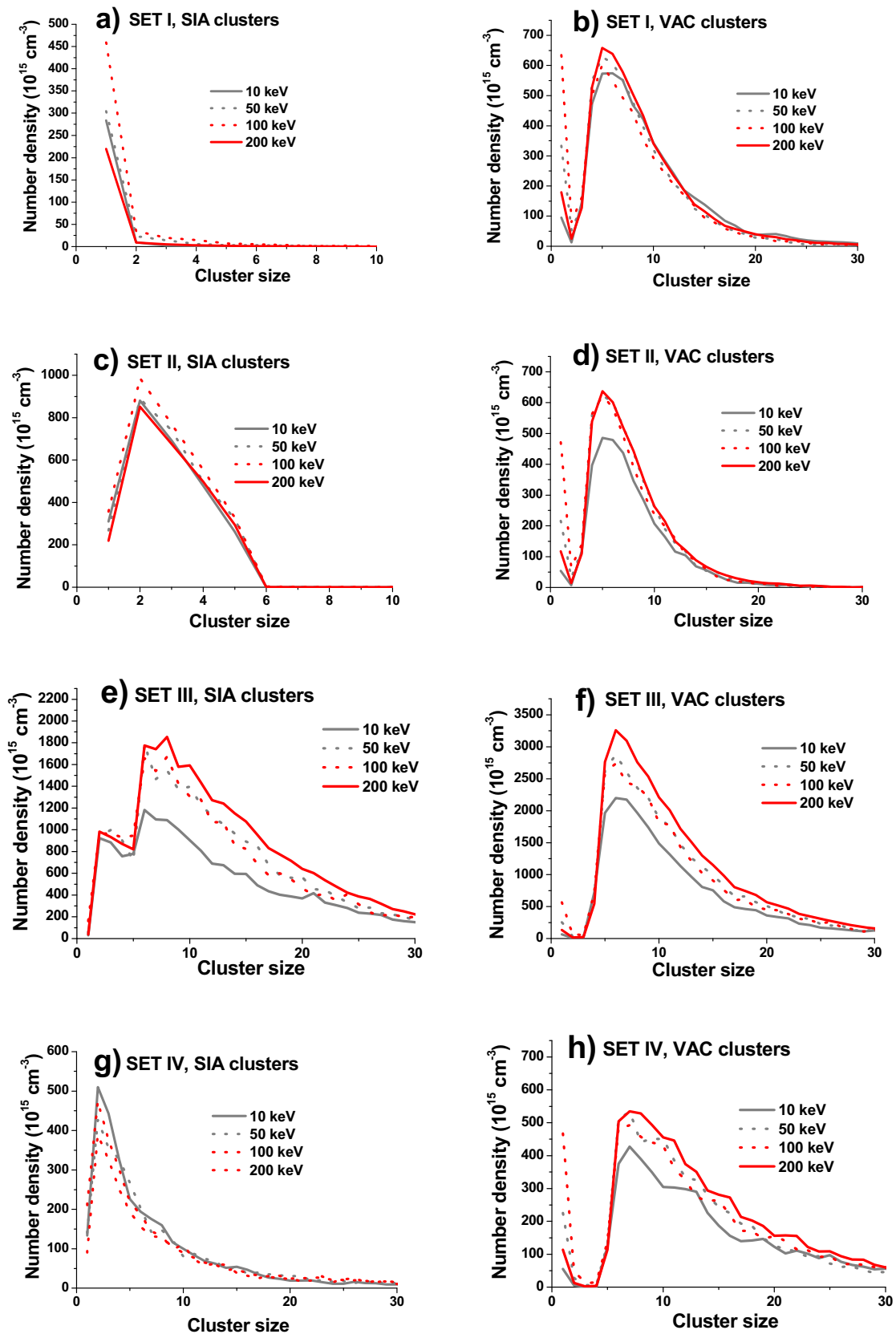


**Fig. 4** Cluster size distributions predicted at the end of 0.1 dpa irradiation as obtained with four sets of OKMC parameters using MD cascades with energies from 10 keV to 200 keV as input. The results obtained with cascades generated by 20, 30, and 40 keV, not represented, are indistinguishable from those obtained at 50 keV. The four sets of parameters were chosen based on certain hypotheses concerning the properties of self-interstitial clusters in iron at that time. They are described in detail in Soudi, A., Hou, M., Becquart, C.S., *et al.*, 2011. On the correlation between primary damage and long-term nanostructural evolution in iron under irradiation. *J. Nucl. Mater.* 419, 122–133. doi:10.1016/j.jnucmat.2011.08.049.

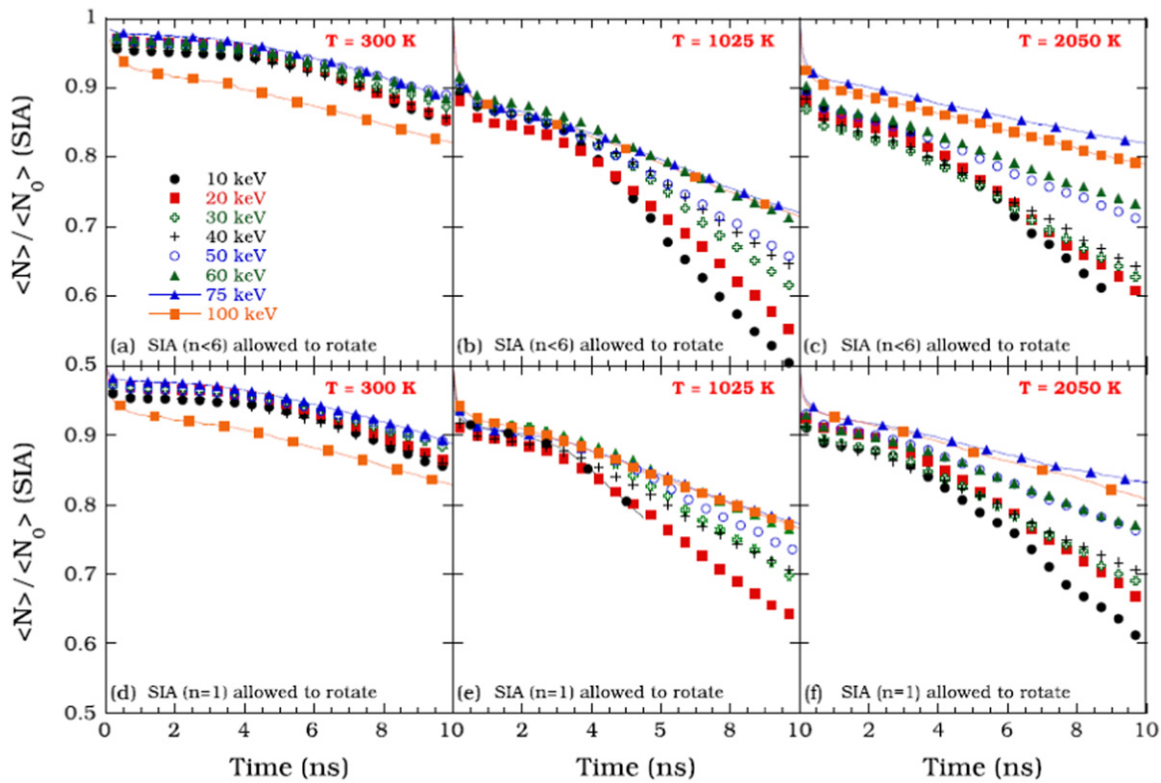


**Fig. 5** Surviving fractions of SIAs as a function of time for different PKA energies at 300, 1025 and 2050K, where all SIA clusters diffuse in 1D. In figure (a)–(c) only small SIA clusters ( $n < 6$ ) rotate. In figure (d)–(f) only mono-SIAs rotate. From Nandipati, G., Setyawan, W., Heinisch, H.L., *et al.*, 2015. Displacement cascades and defect annealing in tungsten, Part III: The sensitivity of cascade annealing in tungsten to the values of kinetic parameters. *J. Nucl. Mater.* 462, 345–353. doi:10.1016/j.jnucmat.2015.01.059.

in particular to investigate the formation of the so-called late blooming phases,<sup>152</sup> phases that are supposed to start to form above a threshold incubation dose in low-Cu, high-Ni (and/or high-Mn) RPV steels, thereby causing additional hardening.

The second most widely investigated binary system is FeCr, model material for high-Cr ferritic/martensitic steels. This system is quite complex as depending upon Cr concentration, precipitation or spinodal decomposition can take place and numerous AKMC simulations have been proposed.<sup>110,153–156</sup> Senninger *et al.*<sup>157</sup> found that the diffusion of vacancies toward sinks leads to a Cr depletion, whereas the diffusion of self-interstitials causes an enrichment of Cr in the vicinity of sinks. The enrichment or depletion of Cr near sinks results from the balance of these two mechanisms and depend thus in a non simple manner on concentration and temperature. A very recent study by Soisson *et al.*<sup>110</sup> (Figs. 7 and 8) pointed out the impact of the sink density on the delicate balance that exists between ballistic mixing and accelerated diffusion on the  $\alpha'$  transformation.

In W, the formation of Re and Os through transmutation has inspired a few KMC (AKMC and OKMC) studies showing the impact of Re and Os on the migration of the SIAs.<sup>118,119</sup> They control the nucleation and the growth of Re-rich clusters and also have a positive impact on swelling and void lattice formation.<sup>103</sup> Radiation induced segregation near extended defects (sinks) such as grain boundaries has also been investigated using KMC.

Other systems have been modeled to study phase transitions or precipitation. We can mention ZrSiO<sub>4</sub>,<sup>158</sup> FeCrAl,<sup>159</sup> Cu<sub>83.5</sub>Ag<sub>15</sub>W<sub>1.5</sub>,<sup>160</sup> Cu-Nb-W,<sup>114</sup> and Cu-W.<sup>161</sup> For a recent review of precipitation modeling by AKMC approaches see 66. Note that a few studies have also been dedicated to investigate the stability of nanoparticles under irradiation and characterize their dissolution.<sup>102,162</sup>

The fate of point defect fluxes migrating towards sinks and their coupling with solutes is one of the most important issue of microstructure evolution under radiation and twenty years of AKMC studies have led to significant results such as the motion of Cu clusters<sup>149</sup> and the synergy between solutes.<sup>146–148</sup> Synergy between solutes makes these studies very difficult as one must find good cohesive models for complex alloys which need not only to be accurate regarding the formation energies of the solute/point defect clusters but also for the migration energies of the point defects in these complex environments. Different approaches are currently being pursued<sup>163</sup> using for instance machine learning, but the task is not trivial, especially for multi-component alloys such as steels. For more simple alloys such as W-Re, or Fe-Cr, AKMC based on a large DFT data base, has really helped in unveiling mechanisms and explaining experimental observations.

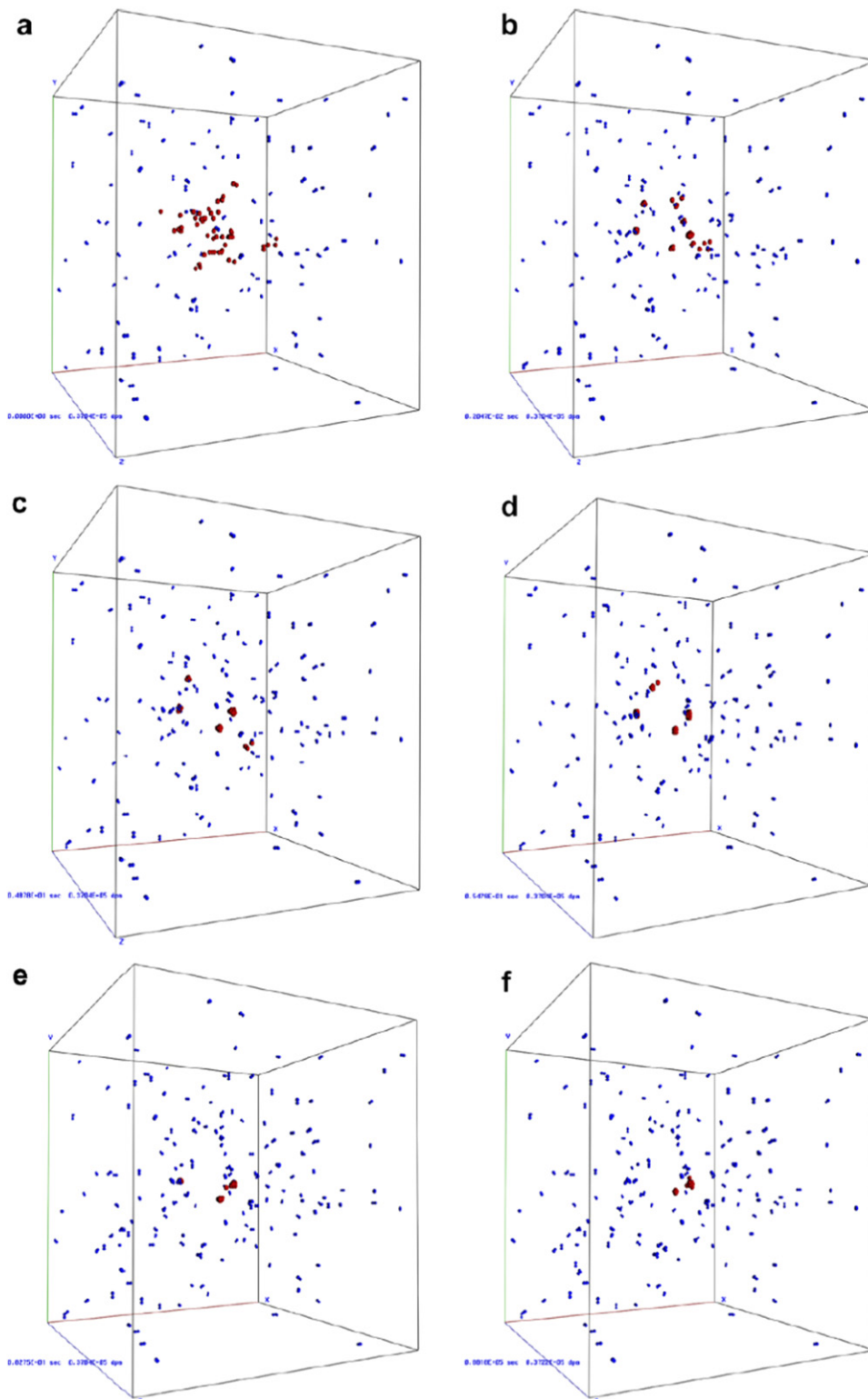


**Fig. 6** Representative vacancy (red circles) and clustered Cu atom (blue circles) evolution in an Fe-0.3% Cu alloy during the aging of a single 20 keV displacement cascade, at (a) initial (200 ns), (b) 2 ms, (c) 48 ms, (d) 55 ms, (e) 83 ms, and (f) 24.5 h. From Monasterio, P.R., Wirth, B.D., Odette, G.R., 2007. Kinetic Monte Carlo modeling of cascade aging and damage accumulation in Fe-Cu alloys. *J. Nucl. Mater.* 361, 127-140. doi:10.1016/j.jnucmat.2006.12.022.

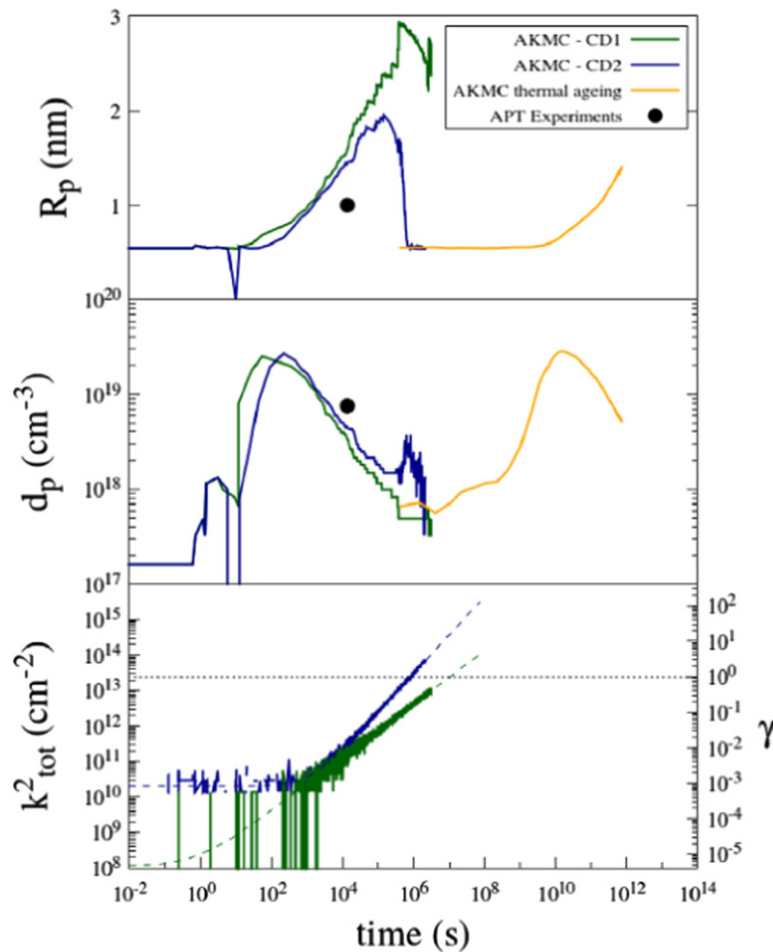


**Fig. 7** Evolution of the average radius and density of  $\alpha'$  precipitates, and of the total sink strength and irradiation intensity in a Fe-15%Cr alloys under ion irradiation at  $5.2 \times 10^{-5}$  dpa  $s^{-1}$  and 300°C. Comparison between APT observations and AKMC simulations. CD1 and CD2 are two sets of parameters for the cluster dynamic method, used to compute the evolution of the sink density/sink strength. From Soisson, F., Meslin, E., Tissot, O., 2018. Atomistic modeling of  $\alpha'$  precipitation in Fe-Cr alloys under charged particles and neutron irradiations: Effects of ballistic mixing and sink densities. *J. Nucl. Mater.* 508, 583–594. doi:10.1016/j.jnucmat.2018.06.015.

#### 1.24.4.3 Typical Damage Accumulation/Microstructure Evolution: Impact of Dose, Temperature, Impurities ...

Many KMC studies have also been dedicated to characterizing damage accumulation in various materials in order to model specific experiments such as ion implantation in Si<sup>164</sup> or to investigate the impact of various parameters. These include: the irradiation technique (ions versus neutrons<sup>165</sup> and heavy ions versus protons<sup>166</sup>; continuous versus pulsed irradiation<sup>167</sup>); the neutron energy spectrum<sup>168,169</sup> (Fig. 9); the dose and dose-rate<sup>168,170</sup>; the temperature,<sup>165,168,170,171</sup> the presence of impurities or solute atoms<sup>127,165,172</sup>; the effect of annealing<sup>166,173</sup>; or to compare different materials.<sup>174</sup>

The irradiation is typically modeled using cascade databases obtained either through MD<sup>165,170,171,173–178</sup> or the BCA method.<sup>75,76,164,179–181</sup> The effect of pulsed irradiation has been studied in Ref. 182 and showed that, in Cu, the impact of the pulse depends on the frequency. Studying the effect of flux,<sup>128</sup> showed that damage accumulation can be, in certain instances (room temperature and light ion implantation), reduced by decreasing the dose rate. The delicate balance between dose-rate and temperature has also been pointed out by Soneda *et al.*<sup>168</sup> This truly underlines the power as well as the weakness of KMC as the fate of the point defects injected by the irradiation cannot be simply deduced from the knowledge of their migration energies and many aspects must be considered. For instance, long term simulations of accumulation of cascades reveal the sensitivity of the system to the properties of the displacement cascades (their spatial extent, morphology and the spatial correlation of defects) in the evolution of point defect cluster size distributions and it was shown that the sensitivity can be low or strongly dependent on other parameters such as the mobility of defects, the type of interactions, the presence of impurities and the temperature.<sup>74,76</sup> A more recent study, comparing the damage accumulation in W obtained using BCA cascades or MD cascades finds that in the case of ion irradiation, BCA results can lead to good OKMC results despite the fact that BCA calculations do not take into account correctly the low energy events taking place in the cascades.<sup>25</sup> However in the case of neutron irradiation, the study predicts that

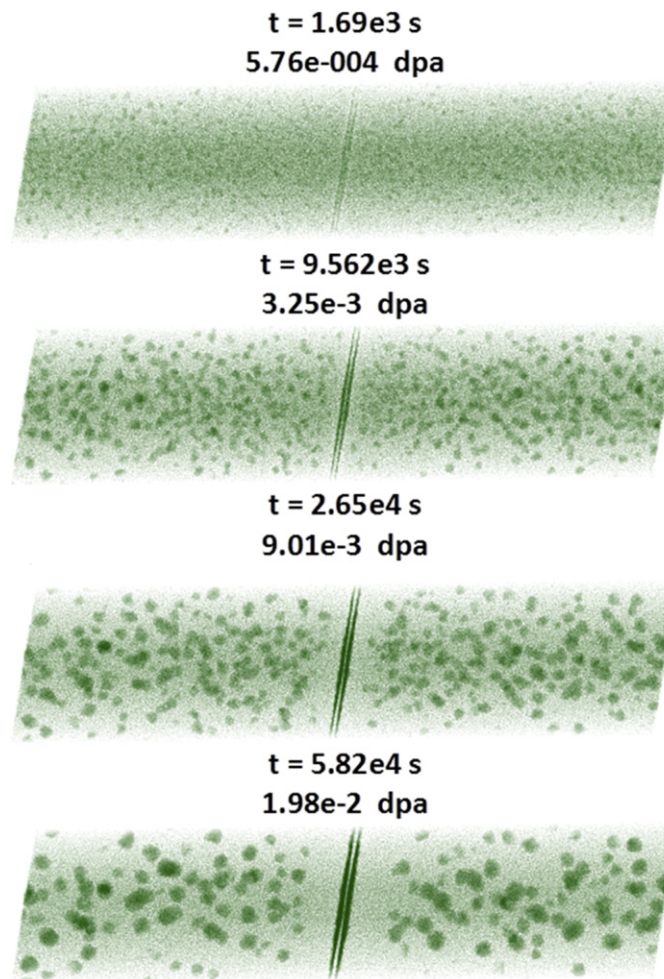


**Fig. 8** AKMC simulations of  $\alpha - \alpha'$  phase separation in Fe-15%Cr under irradiation at 290°C and  $3.4 \times 10^{-7}$  dpa s $^{-1}$ , on the grain boundary and on the neighboring planes. From Soisson, F., Jourdan, T., 2016. Radiation-accelerated precipitation in Fe-Cr alloys. *Acta Mater.* 103, 870–881. doi:10.1016/j.actamat.2015.11.001.

problems may arise when using the BCA cascades as this method overestimates the amount of FP created by high energy PKA<sup>75</sup> and it is thus mandatory to have proper ways of estimating the primary damage.

In the case of semiconductors, the materials are usually simpler, i.e., they do not contain as many alloying elements as structural materials such as steels. However, one has to take into account how electrons and holes distributions evolve along with the point defects. One possibility is to include them in an indirect manner as proposed in Ref. 183. In this approach, vacancies, interstitials, impurities, and reaction-derived species (e.g., impurity/vacancy complexes) are treated as distinct species that are tracked individually as part of the KMC algorithm. Electrons and holes are assumed to exist in certain background concentrations (which depend on position in the device, operating characteristics, etc.), and their interaction rates with defects are quantified through analytic expressions that are functions of the carrier concentrations. These interaction rates are then included in the KMC event selection process, so that defect migration and carrier interaction are both taking place in the simulation. Electrons and holes are thus included in the simulation, but they are not tracked as individual particles that are subject to stochastic behavior. The method was used to model annealing of electron Irradiation of p-Type Silicon and good agreement between the model and the experiment was obtained.<sup>183</sup>

#### 1.24.4.4 Solute or Impurity/Gas Atoms Diffusion and the Formation of Gas Bubbles

Another topic which has been investigated for some time using KMC approaches is the modeling of H and He atoms in structural materials such as Fe and W. This topic is quite important for fusion as structural materials that will be close to the plasma will be bombarded by He and H isotopes. In the case of H and H isotopes, the major concern is to obtain effective diffusion coefficients in the presence of extended defects,<sup>184,185</sup> hydrogen concentration<sup>186</sup> or impurities.<sup>187</sup> Diffusion of H has also been investigated on a W (001) reconstructed surface.<sup>188</sup> In the case of helium, the goal is often to model the

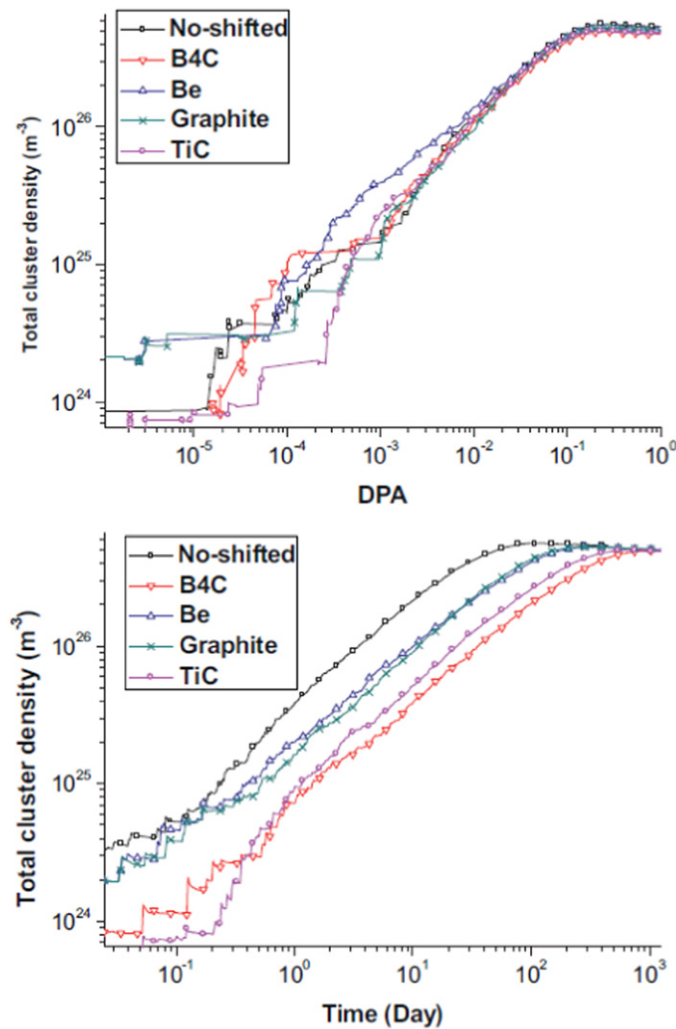


**Fig. 9** DPA and time evolution of total cluster density for different spectral shifters. From Choi, Y.H., Joo, H.G., 2013. Multiscale simulation of neutron induced damage in tritium breeding blankets with different spectral shifters. *Fusion Eng. Des.* 88, 2471–2475. doi:10.1016/j.fusengdes.2013.05.085.

formation of helium vacancy clusters that will be nuclei for voids and bubbles leading to swelling, formation of pores, blistering or exfoliation of the surface and embrittlement. Helium is a very mobile element in metals and forms very stable clusters which are also very mobile unless they are trapped by vacancies or other elements of the microstructure, such as dislocations, grain boundaries, or solute atoms.<sup>189</sup> Predicting the evolution of microstructures implanted with He atoms or containing He atoms is not straightforward as it depends on temperature, point defect and helium implantation rates, dose<sup>190</sup> as well as the way they are implanted (at the same time, or in successive events, continuously or pulsed) or where they are implanted (close or not to free surfaces, i.e., in stress free material or in stress gradients). KMC simulations have investigated the fate of He during co-implantation in Fe and showed that at most 3% end up in vacancies (thus becoming substitutional) in typical implantation set ups.<sup>191</sup> Another study demonstrated the occurrence of different regimes of He cluster nucleation in W, one dominated by He self-trapping (at low temperatures and high implantation rates), the other one, at high temperatures and low implantation rates, where the trapping of helium by vacancies is predominant.<sup>192</sup> Stress gradients due to the presence of surfaces were found to drive collective bubble populations towards the free surface or up the stress gradient<sup>193</sup> (Fig. 10). Comparing continuous He implantation and pulsed He implantation, Rivera *et al.* found that the pulsed modes lead to a higher He retention at high temperature because they produce a higher concentration of defects.<sup>194</sup> Other simulations underline the role of point defects, and in particular the vacancies, and impurities (C for instance) that can trap the He atoms and thus impact on the size distribution of He clusters or on the rate of He desorption.<sup>79,80,195–202</sup> Based on the same ideas that He interacts quite strongly with point defects, other studies focus more on the impact of He atoms on the long term evolution of the primary damage and the formation of voids.<sup>198,203,204</sup> All these studies underline the complex balance between point defect and helium clustering, cluster growth, trapping and detrapping reactions that lead to different microstructure evolutions. Most of these investigations have been done in bcc Fe and W, but a few studies in fcc metals (Fig. 11) and even austenitic steels are available.<sup>199,200,205</sup> A preliminary study comparing the formation of mixed He vacancy

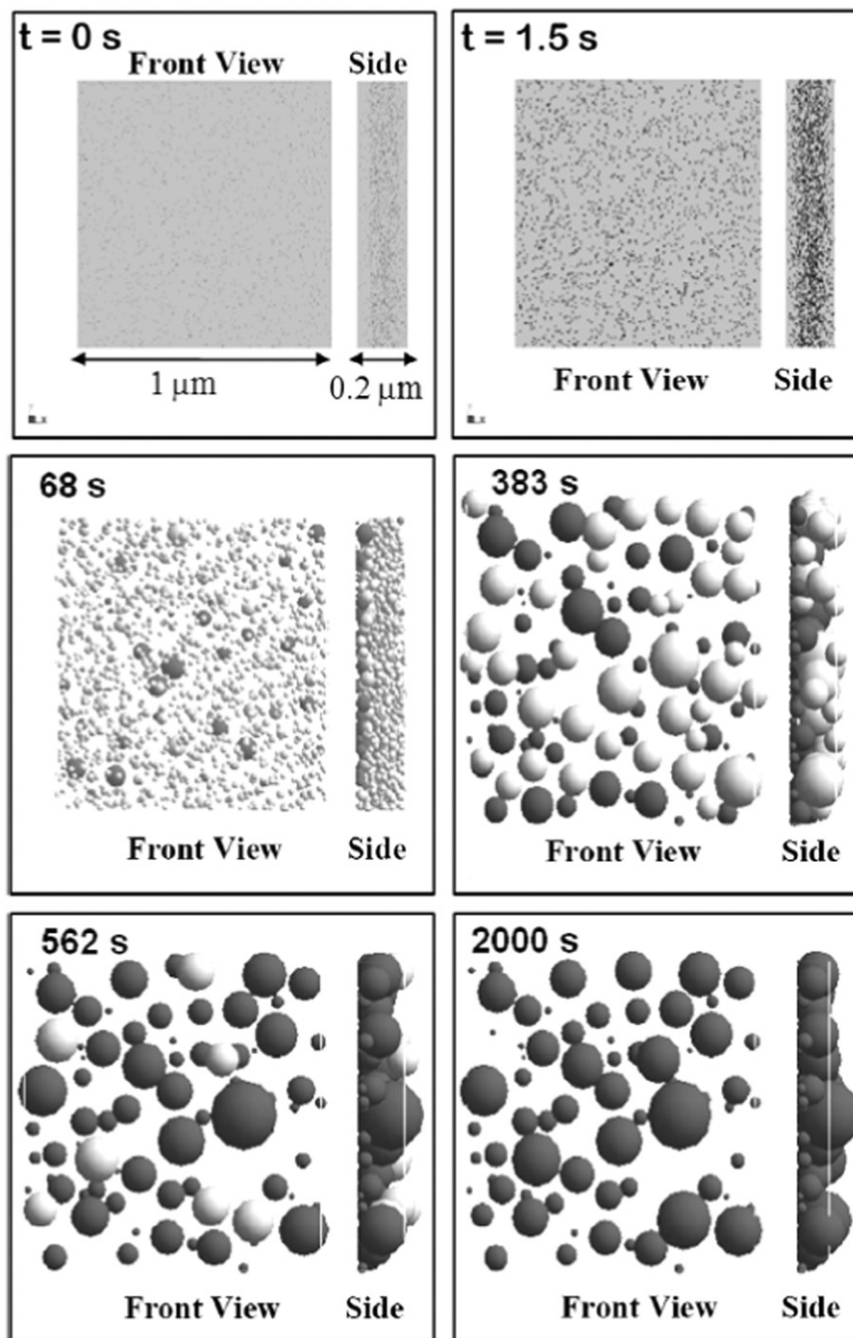


**Fig. 10** Snap shots of the time sequence of the KMC simulation results of the IEC facility at UW-Madison helium implantation condition at  $T = 730^{\circ}\text{C}$ ,  $1.6 \times 10^{18} \text{ He/m}^2 \text{ s}$ ,  $E_{\text{He}} = 30 \text{ keV}$ ; (light colored spheres represent matrix or bulk bubbles; dark spheres represent surface pores or bubbles that have penetrated the top surface). From Sharafat, S., Takahashi, A., Nagasawa, K., Ghoniem, N., 2009. A description of stress driven bubble growth of helium implanted tungsten. *J. Nucl. Mater.* 389, 203–212. doi:10.1016/j.jnucmat.2009.02.027.

clusters in bcc and fcc Fe seems even to find no major difference in clustering behavior.<sup>206</sup> Finally KMC has been used to elucidate the formation of fuzz in W, this peculiar nanostructured morphology, that was shown to result again from the balance between cluster formation and detrapping reactions.<sup>206,207</sup>

In fuel materials, and particularly in  $\text{UO}_2$  it is the diffusion of oxygen and other gases which is mostly being investigated.<sup>208–210</sup> See Ref. 211 for a review paper on the subject. Fission products, such as Ag in TRISO fuels<sup>212</sup> has also been studied, though not really extensively it seems.

The formation and diffusion of gas bubbles has a large impact on structural as well as fuel materials and despite an already quite large amount of studies dedicated to this, more work is needed because of the delicate balance between point defect and gas atom clustering properties that depend, of course, on the matrix and all its solutes or alloying elements but also on internal

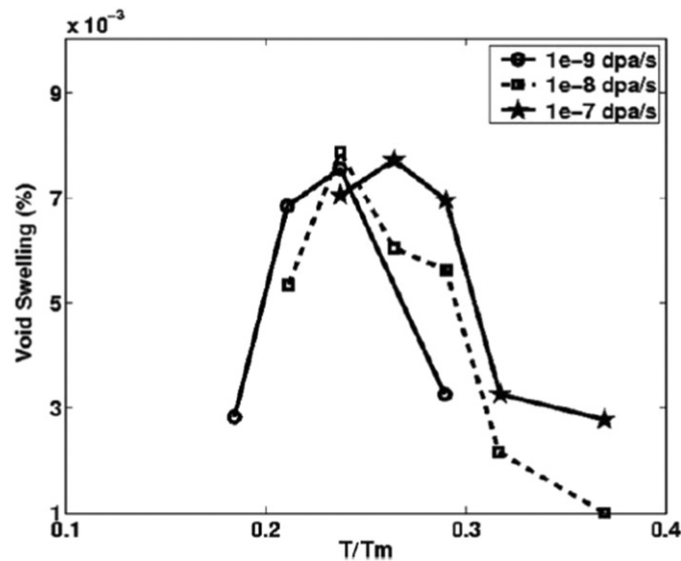


**Fig. 11** Void swelling (or change in volume due to vacancies in He-V complexes) as a function of temperature for a total dose of 0.03 dpa and three different dose rates for damage produced in Au. From Caturla, M.J., Soneda, N., Diaz de la Rubia, T., Fluss, M., 2006. Kinetic Monte Carlo simulations applied to irradiated materials: The effect of cascade damage in defect nucleation and growth. *J. Nucl. Mater.* 351, 78–87. doi:10.1016/j.jnucmat.2006.02.019.



**Fig. 12** Example trajectories at each temperature considered (2500 K, 5000 K, 7500 K, and 10,000 K) for a vacancy diffusing at the R5 tilt GB. There is a clear transition from one-dimensional to two-dimensional motion as the temperature is increased. The direction along the tilt axis is indicated for clarity. The time scale for each simulation is also indicated in the upper left corner of each frame. From Ueberuaga, B.P., Andersson, D.A., 2015. Uranium vacancy mobility at the  $\Sigma 5$  symmetric tilt and  $\Sigma 5$  twist grain boundaries in  $\text{UO}_2$ . *Comput. Mater. Sci.* 108, 80–87. doi:10.1016/j.commatsci.2015.06.017.

pressure, to which they will contribute. In that regard, elastic interactions must be accounted for in the models when bubbles start to grow which adds another level of complexity to the models.

#### 1.24.4.5 Investigating Solutions to Eliminate the Point Defects or Trap Gas Atoms

Radiation damage in metallic alloys consists, as already mentioned, mostly in a large amount of point defects that will diffuse, leading to many changes such as RIS, the formation of solute clusters, the formation of voids and dislocation loops etc. All these features decrease the mechanical properties of the components and solutions are thought to include methods of trapping or eliminating the point defects. In that search, KMC has been used to evaluate the impact of grain boundaries on the fate of point defects in Ni and a Ni-Cr alloy showing that both vacancies and SIAs are attracted to the grain boundaries.<sup>213</sup> A later study, showed that, in Fe, both near GB and at GB, low-energy-barrier/barrier-free regions form around the interstitials, promoting the annihilation of vacancies.<sup>214</sup> Comparing monocrystalline tungsten and nanostructured tungsten, Valles *et al.*<sup>215</sup> confirm the impact of GB on the amount and distribution of vacancies as well as on the migration and retention of H and propose that GB act as preferential path for H. Another study, in Al, showed, on the other hand, that diffusion of H was decreased by more than one order of magnitude in GBs.<sup>216</sup> In  $\text{UO}_2$ , it was found that certain types of grain boundaries enhanced the mobility of U vacancies<sup>217</sup> (Fig. 12). An increase of the diffusivity of Ag and Cs in Tristructural-Isotropic (TRISO) fuel particles in high energy GB as compared to the bulk was also found by Refs. 218,219. The apparent contradictions in these results stem from the fact that depending on several factors such as the grain size, the GB energy, angle, the probability of GB connectivity, and the excess of free volume, GB can be diffusion enhancer or diffusion slower as shown recently in the case of H diffusion in Ni.<sup>220</sup> Martensite laths were investigated

using OKMC simulations and were found not to be the reason for the different nanostructural evolution under neutron irradiation of ferrite and martensite in FeCrC alloys.<sup>221</sup>

Directly related to the issue of trapping/eliminating point defects or gas atoms in extended defects is the determination of the sink strength, a parameter typically used in the Mean Field Rate Theory (MFRT)<sup>222</sup> to describe the interaction of migrating defects with the features characterizing the microstructure of the material (e.g., voids, dislocations, grain boundaries). Because KMC approaches explicitly take into account spatial correlations between the elements of the physical system, they are expected to implicitly reproduce the effect of sinks or traps for migrating species. They have thus been used for more than twenty years to determine the sink strength of various extended defects and compare them to analytical approaches.<sup>94,223–230</sup>

The results summarized above highlight one strength of KMC methods: its capacity to investigate mechanisms at the atomistic level in microstructures containing extended defects on time scales longer than MD. Despite the fact that the results depend on the point defect and point defect clusters mobility, and/or on the cohesive model used, they show where more precise studies should concentrate on. A typical example is the impact of grain boundaries which is more complicated than initially thought as grain boundaries can be seen as containing a large population of defects with rich and largely not understood behavior and impact. Off lattice on-the-fly AKMC should be able to provide valuable information, for systems for which a good cohesive model and a lot of computing time are available. They could help build databases of grain boundary families useful to be integrated in mean-field approaches.

Another family of extended defects which has been barely considered are surfaces, probably because of the difficulty to model, even at the atomistic scale, the complexity of real surfaces (their roughness, the oxide layers, the strain gradients...). Furthermore, reactions occurring at surfaces take place at quite different time scales, which is a problem for KMC techniques similar to the low barrier problem mentioned in Section 1.24.2.2. For some problems, such as the formation of solute clusters under irradiation, surfaces may not be important, for others such as the formation and diffusion of gas bubbles, it will be difficult not to investigate this issue.

### 1.24.5 Comparison of Models

The formation and growth of point defect and solute clusters through all stages of cluster evolution, from their nucleation to growth and coarsening has been extensively simulated by two alternate methods, mean field reaction rate theory (MFRT)<sup>222</sup> and Kinetic Monte Carlo at the mesoscale level, i.e., OKMC. In principle, these two methods should predict essentially the same behavior when used to solve the same problem, if the problem is well posed as shown in Ref. 231 but the comparison is not straightforward and needs to be done very carefully. One important conclusion of the work by Stoller *et al.*<sup>231</sup> is that, because of computational limitations, for the time being, one immediate application of OKMC simulations is to improve the parameterization of the MFRT models as shown in Section 1.24.4.2. A similar conclusion was drawn by Ref. 232 who compared AKMC and MFRT in the modeling of RIS. This situation may evolve as a recent development allowing to speed up KMC simulations enabled Xu *et al.*<sup>233</sup> to model the entire radiation process of molybdenum nanofoils irradiated in a transmission electron microscope.

### 1.24.6 Coupling With Other Methods

To model radiation damage, the different codes necessary to go from the neutron spectra to the evolution of the mechanical or thermal properties of the material<sup>234</sup> are typically used independently. In that scheme, one code provides the input data as shown in Section 1.24.4.3 or in 193 or parameters (DFT and/or MD results concerning the stability and migration of point defects and point defect clusters in KMC models for instance) for the next, in a coarse graining multi-scale approach.<sup>235</sup> However, a few attempts at using different approaches in the same model have been developed. For instance, the OKMC approach is sometimes used within a lower scale method as proposed in Ref. 236 and later Ref. 237 where the AKMC is coupled with the OKMC in the same code, thus producing an hybrid AKMC-OKMC code.<sup>27</sup>

### 1.24.7 Locks/Things That Need to be Investigated/Improved Further

In MD, the determining parameter is the quality of the cohesive model (i.e., the force field or empirical potential) that controls the validity of the thermodynamic and dynamic properties.<sup>238</sup> As a consequence, MD simulations are far from being capable of representing real microstructures that always contain impurities that are not described properly by current force fields. With the help of KMC models, many studies have demonstrated that the mobility of point defects, the stability and mobility of the various objects that can form (point defect clusters, mixed He point defect clusters, dislocations and dislocations loops, etc.), the trapping or slowing down capability of impurities, and the impact of grain boundaries all have tremendous effects. These models are thus capable of providing relevant information that is closer to the scale of real materials. However, these simulations require that a large number of parameters (and the way they evolve with temperature) be known accurately, not to mention the impact of surfaces<sup>239,240</sup> or the source term, as recently shown in Ref. 132. This means that considerable effort must go into choosing the

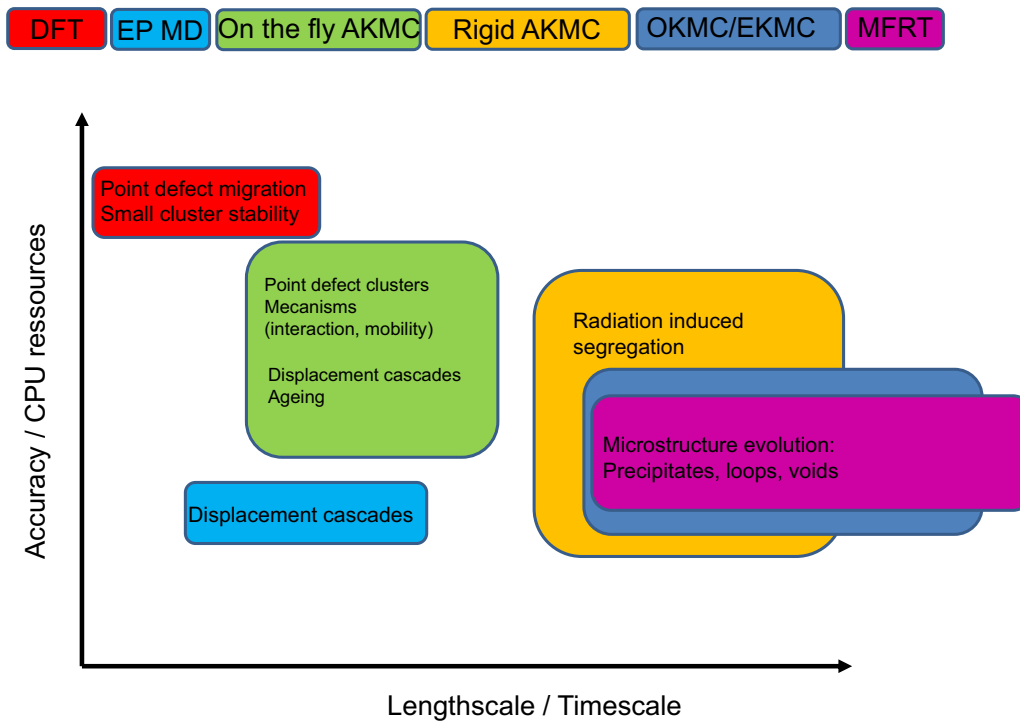


**Fig. 13** Summary of the different KMC approaches compared to DFT and MD with empirical potentials.

level of details to enter in the models to minimally perturb the results. For instance a recent study showed that the additional complexity of size dependent vacancy emission rates from voids had little effect on the defect concentrations.<sup>241</sup> The authors conclude thus that a constant barrier should be sufficient for simulations of voids in bcc metals.

Nevertheless, even if KMC permits modeling the nucleation and growth of larger defects than MD, comparing with experimental data is still a challenge and it is necessary to build tools that link the experimental observations to the objects formed in the simulations. A typical example is the electrical resistivity (ER) method which can provide valuable information on the migration, clustering and dissociation of radiation defects, which are essential for the behavior of materials under irradiation. The ER method has been widely employed due to its high sensitivity, reliability and experimental convenience. Despite the importance of the ER method for radiation damage studies, the quantitative analysis of experimental results is still hindered by the lack of detailed knowledge on the specific contributions from different types of radiation defects, e.g., point-defects, point-defect clusters or defect-impurity complexes to the total resistivity. So far, the crude assumption is made that each point defect (isolated or in cluster) has the same contribution to the electrical resistivity. This is clearly a strong approximation and a better estimate of point defect and point defect cluster residual resistivity will be very helpful to compare the results of KMC and RE models with experiments.

If better experimental data is needed at the atomic level, there are also a number of issues that limit the applications of AKMC. First, the description of the basic kinetic steps, which may be taken from *ab initio*, an empirical description, or a fully phenomenological description. At the moment, no approach provides a general answer, either because costs are too large or the information is not available. There a number of efforts to improve the various levels of description, many involving machine-learning, but the problem remains largely open today. A second and related issue focuses on computing rates accurately, a challenge even with accurate force fields. Given the cost of this step, a number of different approximations have been proposed. Recent simulations suggest that these rates could vary even more than previously thought, which forces a reexamination of many of those used until now. More technically, the reachable simulation time is an important third challenge: many phenomena take place on time scales that are beyond current methods, even if one is ready to wait for days or weeks. To overcome this limitation, efforts have gone, for example, into parallelizing time evolution for large KMC simulations.<sup>242–245</sup> These approaches are technically complex and are limited to relatively simple problems. Other approaches have focused on managing the so-called flickers, i.e., the low-energy barrier mechanisms, to allow rare events to take place. Different methods are being developed to boost the simulation by solving analytically part of the time evolution, see for instance Refs. 246–248. A final challenge is linked to the ability of describing a system in its full complexity, or, at least, with all the complexity needed to address a specific issue. Although progress has been made in understanding the role of impurities, defects, surfaces, strain, etc., introducing structures at many different length scales remains challenging.

Another issue that slows down the simulations is the calculation of the transition rates. Machine learning can speed up these calculations as proposed in Refs. 36–38, as well as be used to help building better cohesive models.<sup>39,249–251</sup>

### 1.24.8 Conclusions

KMC approaches are techniques useful to study generic as well as realistic problems. It provides the link between MD and MFRT (Fig. 13); the AKMC being close to the former, whereas OKMC and EKMC are close to the later. The same algorithm (time residence) can provide different information depending upon the method chosen and the approximations. A typical example is the impact of solutes and alloying elements. In the AKMC approach, solutes are introduced explicitly (a recent review of the different ways of doing so can be found in Ref. 163) and the impact of radiation on the solute distribution can be estimated, and the structure and content of the phases or clusters formed can be obtained. If one chooses the OKMC or EKMC with a grey alloy approach, the structure of the clusters is an entry of the model and not a result and it will not be possible to study phase transitions, whereas it will be possible to study the behavior of point defect fluxes in these alloys on longer time scales than when using AKMC.

The technique has been applied to investigate many issues in the radiation damage community, the most important ones being radiation induced or accelerated phase transformations, the annealing as well as the accumulation of the primary damage with or without gas atom diffusion and the search for solutions to mitigate the damage.

The development of KMC approaches is continuing strongly at the moment at all approximation levels, with advances in the calculation of prefactors, the coupling of various approximations and attempts to use machine learning to facilitate event catalog building, strengthening the capacity of KMC methods to address a wider range of fundamentally and technologically relevant materials questions.

Yet, one of the main outcomes of this article is to underline that using KMC techniques to their best abilities requires that one finds a good compromise between methods (lattice/off lattice; atomic/object) and precision required (for the cohesive model/parameterization) and calculation time. This is indeed similar to many modeling techniques, however because KMC is more flexible and offers a richer set of approximations and tools to choose from than methods such as MD and MFRT, the expertise of the researcher is more crucial. This effort, as we have shown in this article, is well worth it; when they are well used, KMC techniques can clearly provide unique and essential understandings that cannot be achieved with other simulation methods at the moment.

*See also:* 1.04 Radiation-Induced Effects on Microstructure. 1.07 The Effects of Helium in Irradiated Structural Alloys. 1.08 Radiation-Induced Segregation. 1.17 Interatomic Potential Development. 1.18 Molecular Dynamics. 1.19 Binary Collision Approximation. 1.20 Primary Radiation Damage Formation in Solids. 1.23 Reaction Rate Theory. 1.25 Phase Field Methods

### References

1. Wood, W.W., Parker, F.R., 1957. Monte Carlo equation of state of molecules interacting with the Lennard-Jones potential. I. A supercritical isotherm at about twice the critical temperature. *J. Chem. Phys.* 27, 720–733. doi:10.1063/1.1743822.
2. Metropolis, N., Rosenbluth, A.W., Rosenbluth, M.N., *et al.*, 1953. Equation of state calculations by fast computing machines. *J. Chem. Phys.* 21, 1087–1092. doi:10.1063/1.1699114.
3. Besco, D.G., 1967. *Computer Simulation of Point Defect Annealing in Metals*.
4. Doran, D.G., 1970. Computer simulation of displacement spike annealing. *Radiat. Eff.* 2, 249–267. doi:10.1080/00337576908243987.
5. Heinisch, H.L., 1983. Defect production in simulated cascades: Cascade quenching and short-term annealing. *J. Nucl. Mater.* 117, 46–54. doi:10.1016/0022-3115(83)90008-9.
6. Allen, M.P., Tildesley, D.J., 2017. *Computer Simulation of Liquids*, second ed. Oxford University Press.
7. Metropolis, N., Ulam, S., 1949. The Monte Carlo method. *J. Am. Stat. Assoc.* 44, 335–341. doi:10.1080/01621459.1949.10483310.
8. Fichtorn, K.A., Weinberg, W.H., 1991. Theoretical foundations of dynamical Monte Carlo simulations. *J. Chem. Phys.* 95, 1090. doi:10.1063/1.461138.
9. Young, W.M., Elcock, E.W., 1966. Monte Carlo studies of vacancy migration in binary ordered alloys: I. *Proc. Phys. Soc.* 89, 735. doi:10.1088/0370-1328/89/3/329.
10. Vineyard, G.H., 1957. Frequency factors and isotope effects in solid state rate processes. *J. Phys. Chem. Solids* 3, 121–127. doi:10.1016/0022-3697(57)90059-8.
11. Bortz, A.B., Kalos, M.H., Lebowitz, J.L., 1975. A new algorithm for Monte Carlo simulation of Ising spin systems. *J. Comput. Phys.* 17, 10–18. doi:10.1016/0021-9991(75)90060-1.
12. Chatterjee, A., Vlachos, D.G., 2007. An overview of spatial microscopic and accelerated kinetic Monte Carlo methods. *J. Comput. Aided Mater. Des.* 14, 253–308. doi:10.1007/s10820-006-9042-9.
13. Jourdan, T., Fu, C.C., Joly, L., *et al.*, 2011. Direct simulation of resistivity recovery experiments in carbon-doped  $\alpha$ -iron. *Phys. Scr.* 2011, 014049. doi:10.1088/0031-8949/2011/T145/014049.
14. Lanore, J.-M., 1974. Simulation de l'évolution des défauts dans un réseau par le méthode de monte-carlo. *Radiat. Eff.* 22, 153–162. doi:10.1080/10420157408230773.
15. Dalla Torre, J., Bocquet, J.-L., Doan, N.V., *et al.*, 2005. JERK, an event-based Kinetic Monte Carlo model to predict microstructure evolution of materials under irradiation. *Philos. Mag.* 85, 549–558. doi:10.1080/02678370412331320134.
16. Becquart, C.S., Domain, C., 2010. Introducing chemistry in atomistic kinetic Monte Carlo simulations of Fe alloys under irradiation. *Phys. Status Solidi B* 247, 9–22. doi:10.1002/pssb.200945251.
17. Johnson, M.D., Caturla, M.-J., Díaz de la Rubia, T., 1998. A kinetic Monte–Carlo study of the effective diffusivity of the silicon self-interstitial in the presence of carbon and boron. *J. Appl. Phys.* 84, 1963–1967. doi:10.1063/1.368328.
18. Caturla, M.J., Aliaga, M.J., Martin-Bragado, I., *et al.*, 2016. Microstructure evolution in Fe and Fe-Cr alloys with OKMC methods. *EPJ Web Conf.* 115, 03001. doi:10.1051/epjconf/201611503001.
19. Domain, C., Becquart, C.S., Malerba, L., 2004. Simulation of radiation damage in Fe alloys: An object kinetic Monte Carlo approach. *J. Nucl. Mater.* 335, 121–145. doi:10.1016/j.jnucmat.2004.07.037.

20. Martin-Bragado, I., Rivera, A., Valles, G., *et al.*, 2013. MMonCa: An object kinetic Monte Carlo simulator for damage irradiation evolution and defect diffusion. *Comput. Phys. Commun.* 184, 2703–2710. doi:10.1016/j.cpc.2013.07.011.
21. Becquart, C.S., De Backer, A., Domain, C., 2018. *Atomistic Modelling of Radiation Damage in Metallic Alloys*. Hsueh, C.H., Schmauder, S., Chen, C.S. (Eds.), Singapore: Springer.
22. Nordlund, K., Zinkle, S.J., Sand, A.E., *et al.*, 2018. Primary radiation damage: A review of current understanding and models. *J. Nucl. Mater.* 512, 450–479. doi:10.1016/j.jnucmat.2018.10.027.
23. Cai, W., 2020. *Molecular Dynamics*, *Comprehensive Nuclear Materials*, second ed, vol. 1. Elsevier, pp. 573–594.
24. Stoller, R., 2020. *Primary Radiation Damage Formation*, *Comprehensive Nuclear Materials*, second ed, vol. 1. Elsevier, pp. 620–662.
25. Ortiz, C., 2020. *Binary Collision Approximation*, *Comprehensive Nuclear Materials*, second ed, vol. 1. Elsevier, pp. 595–619.
26. Barbu, A., Becquart, C.S., Bocquet, J.L., *et al.*, 2005. Comparison between three complementary approaches to simulate 'large' fluence irradiation: Application to electron irradiation of thin foils. *Philos. Mag.* 85, 541–547. doi:10.1080/14786430412331334616.
27. Domain, C., Becquart, C.S., 2019. Object Kinetic Monte Carlo (OKMC): A coarse-grained approach to radiation damage. In: Andreoni, W., Yip, S. (Eds.), *Handbook of Materials Modeling: Methods: Theory and Modeling*. Cham: Springer International Publishing, pp. 1–26.
28. Van der Ven, A., Ceder, G., Asta, M., Tapesch, P.D., 2001. First-principles theory of ionic diffusion with nondilute carriers. *Phys. Rev. B* 64. doi:10.1103/PhysRevB.64.184307.
29. Vincent, E., Becquart, C.S., Pareige, C., *et al.*, 2008. Precipitation of the FeCu system: A critical review of atomic kinetic Monte Carlo simulations. *J. Nucl. Mater.* 373, 387–401. doi:10.1016/j.jnucmat.2007.06.016.
30. Kang, H.C., Weinberg, W.H., 1989. Dynamic Monte Carlo with a proper energy barrier: Surface diffusion and two-dimensional domain ordering. *J. Chem. Phys.* 90, 2824. doi:10.1063/1.455932.
31. Soisson, F., Barbu, A., Martin, G., 1996. Monte Carlo simulations of copper precipitation in dilute iron-copper alloys during thermal ageing and under electron irradiation. *Acta Mater.* 44, 3789–3800. doi:10.1016/1359-6454(95)00447-5.
32. Sanchez, J.M., Ducastelle, F., Gratias, D., 1984. Generalized cluster description of multicomponent systems. *Phys. Stat. Mech. Appl.* 128, 334–350. doi:10.1016/0378-4371(84)90096-7.
33. Liu, C.L., Odette, G.R., Wirth, B.D., Lucas, G.E., 1997. A lattice Monte Carlo simulation of nanophase compositions and structures in irradiated pressure vessel Fe-Cu-Ni-Mn-Si steels. *Mater. Sci. Eng. A* 238, 202–209. doi:10.1016/S0921-5093(97)00450-4.
34. Ngayam-Happy, R., Olsson, P., Becquart, C.S., Domain, C., 2010. Isochronal annealing of electron-irradiated dilute Fe alloys modelled by an ab initio based AKMC method: Influence of solute–interstitial cluster properties. *J. Nucl. Mater.* 407, 16–28. doi:10.1016/j.jnucmat.2010.07.004.
35. Vincent, E., Becquart, C.S., Domain, C., 2008. Microstructural evolution under high flux irradiation of dilute Fe–CuNiMnSi alloys studied by an atomic kinetic Monte Carlo model accounting for both vacancies and self interstitials. *J. Nucl. Mater.* 382, 154–159. doi:10.1016/j.jnucmat.2008.08.019.
36. Castin, N., Malerba, L., 2010. Calculation of proper energy barriers for atomistic kinetic Monte Carlo simulations on rigid lattice with chemical and strain field long-range effects using artificial neural networks. *J. Chem. Phys.* 132, 074507. doi:10.1063/1.3298990.
37. Djurabekova, F., Malerba, L., Pasianot, R.C., *et al.*, 2010. Kinetics versus thermodynamics in materials modeling: The case of the di-vacancy in iron. *Philos. Mag.* 90, 2585–2595. doi:10.1080/14786431003662515.
38. Domingos, R.P., Cerchiara, G.M., Djurabekova, F., Malerba, L., 2006. Artificial intelligence applied to simulation of radiation damage in ferritic alloys. *Appl. Artif. Intell.* 883–890.
39. Ackland, G., 2020. *Interatomic Potential Development*, *Comprehensive Nuclear Materials*, second ed. Elsevier, vol. 1, pp. 544–572.
40. Henkelman, G., Jónsson, H., 2001. Long time scale kinetic Monte Carlo simulations without lattice approximation and predefined event table. *J. Chem. Phys.* 115, 9657. doi:10.1063/1.1415500.
41. Trushin, O., Karim, A., Kara, A., Rahman, T.S., 2005. Self-learning kinetic Monte Carlo method: Application to Cu(111). *Phys. Rev. B* 72, 115401. doi:10.1103/PhysRevB.72.115401.
42. El-Mellouhi, F., Mousseau, N., Lewis, L.J., 2008. Kinetic activation-relaxation technique: An off-lattice self-learning kinetic Monte Carlo algorithm. *Phys. Rev. B* 78, 153202. doi:10.1103/PhysRevB.78.153202.
43. Barkema, G.T., Mousseau, N., 1996. Event-based relaxation of continuous disordered systems. *Phys. Rev. Lett.* 77, 4358–4361. doi:10.1103/PhysRevLett.77.4358.
44. Malek, R., Mousseau, N., 2000. Dynamics of Lennard-Jones clusters: A characterization of the activation-relaxation technique. *Phys. Rev. E* 62, 7723–7728. doi:10.1103/PhysRevE.62.7723.
45. McKay, B.D., 1981. Practical graph isomorphism. *Congr. Numer.* 30, 45–87.
46. McKay, B.D., Piperno, A., 2014. Practical graph isomorphism, II. *J. Symb. Comput.* 60, 94–112. doi:10.1016/j.jsc.2013.09.003.
47. Joly, J.-F., Béland, L.K., Brommer, P., *et al.*, 2012. Optimization of the kinetic activation-relaxation technique, an off-lattice and self-learning kinetic Monte-Carlo method. *J. Phys. Conf. Ser.* 341, 012007. doi:10.1088/1742-6596/341/1/012007.
48. Béland, L.K., Anahory, Y., Smeets, D., *et al.*, 2013. Replenish and relax: Explaining logarithmic annealing in ion-implanted c-Si. *Phys. Rev. Lett.* 111, 105502. doi:10.1103/PhysRevLett.111.105502.
49. Béland, L.K., Brommer, P., El-Mellouhi, F., *et al.*, 2011. Kinetic activation-relaxation technique. *Phys. Rev. E* 84, 046704. doi:10.1103/PhysRevE.84.046704.
50. Brommer, P., Béland, L.K., Joly, J.-F., Mousseau, N., 2014. Understanding long-time vacancy aggregation in iron: A kinetic activation-relaxation technique study. *Phys. Rev. B* 90, 134109. doi:10.1103/PhysRevB.90.134109.
51. Trochet, M., Béland, L.K., Joly, J.-F., *et al.*, 2015. Diffusion of point defects in crystalline silicon using the kinetic activation-relaxation technique method. *Phys. Rev. B* 91, 224106. doi:10.1103/PhysRevB.91.224106.
52. Mahmoud, S., Trochet, M., Restrepo, O.A., Mousseau, N., 2018. Study of point defects diffusion in nickel using kinetic activation-relaxation technique. *Acta Mater.* 144, 679–690. doi:10.1016/j.actamat.2017.11.021.
53. Xu, H., Stoller, R.E., Osetsky, Y.N., Terentyev, D., 2013. Solving the puzzle of  $\langle 100 \rangle$  interstitial loop formation in bcc iron. *Phys. Rev. Lett.* 110, 265503. doi:10.1103/PhysRevLett.110.265503.
54. Restrepo, O.A., Mousseau, N., Trochet, M., *et al.*, 2018. Carbon diffusion paths and segregation at high-angle tilt grain boundaries in  $\alpha$ -Fe studied by using a kinetic activation-relaxation technique. *Phys. Rev. B* 97, 054309. doi:10.1103/PhysRevB.97.054309.
55. Xu, H., Osetsky, Y.N., Stoller, R.E., 2011. Simulating complex atomistic processes: On-the-fly kinetic Monte Carlo scheme with selective active volumes. *Phys. Rev. B* 84. doi:10.1103/PhysRevB.84.132103.
56. Béland, L.K., Osetsky, Y.N., Stoller, R.E., Xu, H., 2015. Kinetic activation–relaxation technique and Self-Evolving Atomistic Kinetic Monte Carlo: Comparison of on-the-fly Kinetic Monte Carlo algorithms. *Comput. Mater. Sci.* 100, 124–134. doi:10.1016/j.commatsci.2014.12.001.
57. Nakashima, K., Stoller, R.E., Xu, H., 2015. Recombination radius of a Frenkel pair and capture radius of a self-interstitial atom by vacancy clusters in bcc Fe. *J. Phys. Condens. Matter* 27, 335401. doi:10.1088/0953-8984/27/33/335401.
58. Chill, S.T., Henkelman, G., 2014. Molecular dynamics saddle search adaptive kinetic Monte Carlo. *J. Chem. Phys.* 140, 214110. doi:10.1063/1.4880721.
59. Swinburne, T.D., Marinica, M.-C., 2018. Unsupervised calculation of free energy barriers in large crystalline systems. *Phys. Rev. Lett.* 120, 135503. doi:10.1103/PhysRevLett.120.135503.
60. Uberuaga, B.P., Perez, D., 2018. Computational methods for long-timescale atomistic simulations. In: Andreoni, W., Yip, S. (Eds.), *Handbook of Materials Modeling: Methods: Theory and Modeling*. Cham: Springer International Publishing, pp. 1–6.

61. Voter, A.F., Montalenti, F., Germann, T.C., 2002. Extending the time scale in atomistic simulation of materials. *Annu. Rev. Mater. Res.* 32, 321–346. doi:10.1146/annurev.matsci.32.112601.141541.
62. Henkelman, G., Jónsson, H., Lelièvre, T., *et al.*, 2018. Long-timescale simulations: Challenges, pitfalls, best practices, for development and applications. In: Andreoni, W., Yip, S. (Eds.), *Handbook of Materials Modeling: Methods: Theory and Modeling*. Cham: Springer International Publishing, pp. 1–10.
63. Martínez-Martínez, D., Herdes, C., Vega, L.F., 2018. Crystallization processes in bicomponent thin film depositions: Towards a realistic kinetic Monte Carlo simulation. *Surf. Coat. Technol.* 343, 38–48. doi:10.1016/j.surfcoat.2017.11.022.
64. Fujii, T., Tohgo, K., Kenmochi, A., Shimamura, Y., 2015. Experimental and numerical investigation of stress corrosion cracking of sensitized type 304 stainless steel under high-temperature and high-purity water. *Corros. Sci.* 97, 139–149. doi:10.1016/j.corsci.2015.05.001.
65. Herbert, F.W., Krishnamoorthy, A., Ma, W., *et al.*, 2014. Dynamics of point defect formation, clustering and pit initiation on the pyrite surface. *Electrochim. Acta* 127, 416–426. doi:10.1016/j.electacta.2014.02.048.
66. Bequart, C.S., Soisson, F., 2018. Monte Carlo simulations of precipitation under irradiation. In: Schmauder, S., Chen, C.-S., Chawla, K.K., *et al.* (Eds.), *Handbook of Mechanics of Materials*. Singapore: Springer, pp. 1–29.
67. Zinkle, S.J., 2020. Radiation-Induced Effects on Microstructure, *Comprehensive Nuclear Materials*, second ed, vol. 1. Elsevier, pp. 91–129.
68. Norgett, M.J., Robinson, M.T., Torrens, I.M., 1975. A proposed method of calculating displacement dose rates. *Nucl. Eng. Des.* 33, 50–54. doi:10.1016/0029-5493(75)90035-7.
69. ASTM E693, 1994. *Annual Book of ASTM Standards*. Philadelphia, PA: ASTM.
70. Ziegler, J.F., Ziegler, M.D., Biersack, J.P., 2010. SRIM – The stopping and range of ions in matter (2010). *Nucl. Instrum. Methods Phys. Res. Sect. B Beam Interact. Mater. At.* 268, 1818–1823. doi:10.1016/j.nimb.2010.02.091.
71. Robinson, M.T., 1989. Slowing-down time of energetic atoms in solids. *Phys. Rev. B* 40, 10717–10726. doi:10.1103/PhysRevB.40.10717.
72. Bequart, C.S., Domain, C., Malerba, L., Hou, M., 2005. The influence of the internal displacement cascades structure on the growth of point defect clusters in radiation environment. *Nucl. Instrum. Methods Phys. Res. Sect. B Beam Interact. Mater. At.* 228, 181–186. doi:10.1016/j.nimb.2004.10.031.
73. Souidi, A., Bequart, C.S., Domain, C., *et al.*, 2006. Dependence of radiation damage accumulation in iron on underlying models of displacement cascades and subsequent defect migration. *J. Nucl. Mater.* 355, 89–103. doi:10.1016/j.jnucmat.2006.04.009.
74. Souidi, A., Hou, M., Bequart, C.S., *et al.*, 2011. On the correlation between primary damage and long-term nanostructural evolution in iron under irradiation. *J. Nucl. Mater.* 419, 122–133. doi:10.1016/j.jnucmat.2011.08.049.
75. Valles, G., Cazalilla, A.L., Gonzalez, C., *et al.*, 2015. A multiscale approach to defect evolution in tungsten under helium irradiation. *Nucl. Instrum. Methods Phys. Res. Sect. B Beam Interact. Mater. At.* 352, 100–103. doi:10.1016/j.nimb.2014.12.034.
76. Bequart, C.S., Souidi, A., Domain, C., *et al.*, 2006. Effect of displacement cascade structure and defect mobility on the growth of point defect clusters under irradiation. *J. Nucl. Mater.* 351, 39–46. doi:10.1016/j.jnucmat.2006.02.022.
77. Caturla, M.J., Soneda, N., Diaz de la Rubia, T., Fluss, M., 2006. Kinetic Monte Carlo simulations applied to irradiated materials: The effect of cascade damage in defect nucleation and growth. *J. Nucl. Mater.* 351, 78–87. doi:10.1016/j.jnucmat.2006.02.019.
78. Soisson, F., 2006. Kinetic Monte Carlo simulations of radiation induced segregation and precipitation. *J. Nucl. Mater.* 349, 235–250. doi:10.1016/j.jnucmat.2005.11.003.
79. Bequart, C.S., Domain, C., 2009. An object Kinetic Monte Carlo Simulation of the dynamics of helium and point defects in tungsten. *J. Nucl. Mater.* 385, 223–227. doi:10.1016/j.jnucmat.2008.11.027.
80. Caturla, M.J., Ortiz, C.J., Fu, C.C., 2008. Helium and point defect accumulation: (ii) kinetic modelling. *Comptes Rendus Phys.* 9, 401–408. doi:10.1016/j.crhy.2007.09.004.
81. Soneda, N., de la Rubia, T.D., 1998. Defect production, annealing kinetics and damage evolution in  $\alpha$ -Fe: An atomic-scale computer simulation. *Philos. Mag. A* 78, 995–1019. doi:10.1080/01418619808239970.
82. Nastar, M., 2020. Radiation-Induced Segregation, *Comprehensive Nuclear Materials*, second ed, vol. 1. Elsevier, pp. 235–264.
83. Samolyuk, G.D., Barashev, A.V., Golubov, S.I., *et al.*, 2014. Analysis of the anisotropy of point defect diffusion in hcp Zr. *Acta Mater.* 78, 173–180. doi:10.1016/j.actamat.2014.06.024.
84. Meslin, E., Barbu, A., Boulanger, L., *et al.*, 2008. Cluster-dynamics modelling of defects in  $\alpha$ -iron under cascade damage conditions. *J. Nucl. Mater.* 382, 190–196. doi:10.1016/j.jnucmat.2008.08.010.
85. Meslin, E., Lambrecht, M., Hernández-Mayoral, M., *et al.*, 2010. Characterization of neutron-irradiated ferritic model alloys and a RPV steel from combined APT, SANS, TEM and PAS analyses. *J. Nucl. Mater.* 406, 73–83. doi:10.1016/j.jnucmat.2009.12.021.
86. Yi, X., Jenkins, M.L., Hattar, K., *et al.*, 2015. Characterisation of radiation damage in W and W-based alloys from 2 MeV self-ion near-bulk implantations. *Acta Mater.* 92, 163–177. doi:10.1016/j.actamat.2015.04.015.
87. Hernández-Mayoral, M., Gómez-Briceño, D., 2010. Transmission electron microscopy study on neutron irradiated pure iron and RPV model alloys. *J. Nucl. Mater.* 399, 146–153. doi:10.1016/j.jnucmat.2009.11.013.
88. Bacon, D.J., Osetsyky, Y.N., Rodney, D., 2009. Chapter 88 – Dislocation–obstacle interactions at the atomic level. In: *Dislocations in Solids*. Elsevier, pp. 1–90.
89. Arakawa, K., Ono, K., Isshiki, M., *et al.*, 2007. Observation of the one-dimensional diffusion of nanometer-sized dislocation loops. *Science* 318, 956–959. doi:10.1126/science.1145386.
90. Wen, M., Takahashi, A., Ghoniem, N.M., 2009. Kinetics of self-interstitial cluster aggregation near dislocations and their influence on hardening. *J. Nucl. Mater.* 392, 386–395. doi:10.1016/j.jnucmat.2008.10.029.
91. Ghoniem, N.M., Tong, S.H., Huang, J., *et al.*, 2002. Mechanisms of dislocation-defect interactions in irradiated metals investigated by computer simulations. *J. Nucl. Mater.* 307–311, 843–851. doi:10.1016/S0022-3115(02)01092-9.
92. Heinisch, H.L., Singh, B.N., Golubov, S.I., 2000. Kinetic Monte Carlo studies of the effects of Burgers vector changes on the reaction kinetics of one-dimensionally gliding interstitial clusters. *J. Nucl. Mater.* 276, 59–64. doi:10.1016/S0022-3115(99)00169-5.
93. Heinisch, H.L., Singh, B.N., Golubov, S.I., 1999. Kinetic Monte Carlo study of mixed 1D/3D defect migration. *J. Comput. Aided Mater. Des.* 6, 277–282.
94. Jansson, V., Malerba, L., De Backer, A., *et al.*, 2013. Sink strength calculations of dislocations and loops using OKMC. *J. Nucl. Mater.* 442, 218–226. doi:10.1016/j.jnucmat.2013.08.052.
95. Amino, T., Arakawa, K., Mori, H., 2011. Reaction rate between 1D migrating self-interstitial atoms: An examination by kinetic Monte Carlo simulation. *Philos. Mag.* 91, 3276–3289. doi:10.1080/14786435.2011.575411.
96. Béland, L.K., Osetsyky, Y.N., Stoller, R.E., Xu, H., 2015. Interstitial loop transformations in FeCr. *J. Alloy. Compd.* 640, 219–225. doi:10.1016/j.jallcom.2015.03.173.
97. Domain, C., Bequart, C.S., 2018. Solute –  $\langle 111 \rangle$  interstitial loop interaction in  $\alpha$ -Fe: A DFT study. *J. Nucl. Mater.* 499, 582–594. doi:10.1016/j.jnucmat.2017.10.070.
98. Hudson, T.S., Dudarev, S.L., Sutton, A.P., 2004. Suppression of interstitial cluster diffusion by oversized solute atoms. *J. Nucl. Mater.* 329–333, 971–976. doi:10.1016/j.jnucmat.2004.04.066.
99. Chiappetto, M., Bequart, C.S., Domain, C., Malerba, L., 2015. Nanostructure evolution under irradiation of Fe(C)MnNi model alloys for reactor pressure vessel steels. *Nucl. Instrum. Methods Phys. Res. Sect. B Beam Interact. Mater. At.* 352, 56–60. doi:10.1016/j.nimb.2014.11.102.
100. Terentyev, D., Martín-Bragado, I., 2015. Evolution of dislocation loops in iron under irradiation: The impact of carbon. *Scr. Mater.* 97, 5–8. doi:10.1016/j.scriptamat.2014.10.021.
101. Lee, G.-G., Kwon, J., Kim, D.S., 2009. A kinetic Monte Carlo approach for the analysis of trapping effect on the defect accumulation in neutron-irradiated Fe. *Nucl. Instrum. Methods Phys. Res. Sect. B Beam Interact. Mater. At.* 267, 3214–3217. doi:10.1016/j.nimb.2009.06.063.

102. Gámez, L., Gámez, B., Caturla, M.J., *et al.*, 2011. Object Kinetic Monte Carlo calculations of irradiated Fe–Cr dilute alloys: The effect of the interaction radius between substitutional Cr and self-interstitial Fe. *Nucl. Instrum. Methods Phys. Res. Sect. B Beam Interact. Mater. At.* 269, 1684–1688. doi:10.1016/j.nimb.2010.12.044.
103. Bonny, G., Castin, N., BakaeV, A., Terentyev, D., 2018. Kinetic Monte Carlo model for 1-D migration in a field of strong traps: Application to self-interstitial clusters in W-Re alloys. *Comput. Mater. Sci.* 144, 355–362. doi:10.1016/j.commatsci.2017.12.024.
104. Hudson, T.S., Dudarev, S.L., Caturla, M.-J., Sutton, A.P., 2005. Effects of elastic interactions on post-cascade radiation damage evolution in kinetic Monte Carlo simulations. *Philos. Mag.* 85, 661–675. doi:10.1080/14786430412331320026.
105. Mason, D.R., Yi, X., Kirk, M.A., Dudarev, S.L., 2014. Elastic trapping of dislocation loops in cascades in ion-irradiated tungsten foils. *J. Phys. Condens. Matter* 26, 375701. doi:10.1088/0953-8984/26/37/375701.
106. Wen, M., Ghoniem, N.M., Singh, B.N., 2005. Dislocation decoration and raft formation in irradiated materials. *Philos. Mag.* 85, 2561–2580. doi:10.1080/14786430500154281.
107. Messina, L., Malerba, L., Olsson, P., 2015. Stability and mobility of small vacancy–solute complexes in Fe–MnNi and dilute Fe–X alloys: A kinetic Monte Carlo study. *Nucl. Instrum. Methods Phys. Res. Sect. B Beam Interact. Mater. At.* 352, 61–66. doi:10.1016/j.nimb.2014.12.032.
108. Krasnochtchekov, P., Averback, R.S., Bellon, P., 2007. Precipitate stability and morphology in irradiation environments. *JOM* 59, 46–50. doi:10.1007/s11837-007-0054-z.
109. Krasnochtchekov, P., Averback, R.S., Bellon, P., 2007. Homogeneous phase separation in binary alloys under ion irradiation conditions: Role of interstitial atoms. *Phys. Rev. B* 75, 144107. doi:10.1103/PhysRevB.75.144107.
110. Soisson, F., Meslin, R.A., Tissot, O., 2018. Atomistic modeling of a' precipitation in Fe-Cr alloys under charged particles and neutron irradiations: Effects of ballistic mixing and sink densities. *J. Nucl. Mater.* 508, 583–594. doi:10.1016/j.jnucmat.2018.06.015.
111. Vu, T.H.Y., Ramjaun, Y., Rizza, G., Hayoun, M., 2016. Effect of the size of nanoparticles on their dissolution within metal-glass nanocomposites under sustained irradiation. *J. Appl. Phys.* 119, 034302. doi:10.1063/1.4939974.
112. Martin, G., Bellon, P., 1996. Driven alloys. In: Spaepen, F., Ehrenreich, H. (Eds.), *Solid State Physics. Academic Press*, pp. 189–331.
113. Ye, J., Bellon, P., 2004. Nanoscale patterning of chemical order induced by displacement cascades in irradiated alloys. I. A kinetic Monte Carlo study. *Phys. Rev. B* 70, 094104. doi:10.1103/PhysRevB.70.094104.
114. Bellon, P., Averback R.S., 2015. *Self-Organization Reactions Under Irradiation: Toward the Design of Radiation-Resistant Materials*, pp. 873–874.
115. Bellon, P., Enrique, R.A., 2001. Interface stability and self-organization of precipitates under irradiation. *Nucl. Instrum. Methods Phys. Res. Sect. B Beam Interact. Mater. At.* 178, 1–6. doi:10.1016/S0168-583X(00)00500-0.
116. Lear, C.R., Bellon, P., Averback, R.S., 2017. Novel mechanism for order patterning in alloys driven by irradiation. *Phys. Rev. B* 96, 104108. doi:10.1103/PhysRevB.96.104108.
117. Gilbert, M.R., Sublet, J.-C., 2011. Neutron-induced transmutation effects in W and W- $\alpha$  alloys in a fusion environment. *Nucl. Fusion* 51 (043005), doi:10.1088/0029-5515/51/4/043005.
118. Suzudo, T., Yamaguchi, M., Hasegawa, A., 2015. Migration of rhenium and osmium interstitials in tungsten. *J. Nucl. Mater.* 467, 418–423. doi:10.1016/j.jnucmat.2015.05.051.
119. Huang, C.-H., Gharaee, L., Zhao, Y., *et al.*, 2017. Mechanism of nucleation and incipient growth of Re clusters in irradiated W-Re alloys from kinetic Monte Carlo simulations. *Phys. Rev. B* 96, 094108. doi:10.1103/PhysRevB.96.094108.
120. Kittiratanawasin, L., Smith, R., Uberuaga, B.P., Sickafus, K.E., 2009. Radiation damage and evolution of radiation-induced defects in Er<sub>2</sub>O<sub>3</sub> bixbyite. *J. Phys. Condens. Matter* 21, 115403. doi:10.1088/0953-8984/21/11/115403.
121. Pelaz, L., Marqués, L.A., López, P., *et al.*, 2007. Multiscale modeling of radiation damage and annealing in Si. *Nucl. Instrum. Methods Phys. Res. Sect. B Beam Interact. Mater. At.* 255, 95–100. doi:10.1016/j.nimb.2006.11.035.
122. Suzudo, T., Golubov, S.I., Stoller, R.E., *et al.*, 2012. Annealing simulation of cascade damage in a-Fe – Damage energy and temperature dependence analyses. *J. Nucl. Mater.* 423, 40–46. doi:10.1016/j.jnucmat.2012.01.014.
123. Wu, G.-Y., Hu, N.-W., Deng, H.-Q., *et al.*, 2017. Simulation of radiation damages in molybdenum by combining molecular dynamics and OKMC. *Nucl. Sci. Tech.* 28, 3. doi:10.1007/s41365-016-0164-9.
124. Xiao, W.-J., Wu, G.-Y., Li, M.-H., *et al.*, 2016. MD and OKMC simulations of the displacement cascades in nickel. *Nucl. Sci. Tech.* 27, 57. doi:10.1007/s41365-016-0057-y.
125. Xu, H., Osetsy, Y.N., Stoller, R.E., 2012. Cascade annealing simulations of bcc iron using object kinetic Monte Carlo. *J. Nucl. Mater.* 423, 102–109. doi:10.1016/j.jnucmat.2012.01.020.
126. Yoshiie, T., Ito, T., Iwase, H., *et al.*, 2011. Multi-scale modeling of irradiation effects in spallation neutron source materials. *Nucl. Instrum. Methods Phys. Res. Sect. B Beam Interact. Mater. At.* 269, 1740–1743. doi:10.1016/j.nimb.2010.11.076.
127. Alonso, E., Caturla, M.-J., Di'az de la Rubia, T., Perlado, J.M., 2000. Simulation of damage production and accumulation in vanadium. *J. Nucl. Mater.* 276, 221–229. doi:10.1016/S0022-3115(99)00181-6.
128. Diaz, D.L.R., Soneida, N., Caturla, M.J., Alonso, E.A., 1997. Defect production and annealing kinetics in elemental metals and semiconductors. *J. Nucl. Mater.* 251, 13–33.
129. Gao, F., Bacon, D.J., Barashev, A.V., Heinisch, H.L., 1999. Kinetic Monte Carlo annealing simulation of damage produced by cascades in alpha-iron. *Mater. Res. Soc. Symp. Proc.* 540, 703–708.
130. Adjanor, G., Bugat, S., Domain, C., Barbu, A., 2010. Overview of the RPV-2 and INTERN-1 packages: From primary damage to microplasticity. *J. Nucl. Mater.* 406, 175–186. doi:10.1016/j.jnucmat.2009.09.006.
131. Jourdan, T., Crocombette, J.-P., 2012. Rate theory cluster dynamics simulations including spatial correlations within displacement cascades. *Phys. Rev. B* 86, 054113. doi:10.1103/PhysRevB.86.054113.
132. Jourdan, T., Crocombette, J.-P., 2018. On the transfer of cascades from primary damage codes to rate equation cluster dynamics and its relation to experiments. *Comput. Mater. Sci.* 145, 235–243. doi:10.1016/j.commatsci.2018.01.009.
133. Nandipati, G., Setyawan, W., Heinisch, H.L., *et al.*, 2015. Displacement cascades and defect annealing in tungsten, Part II: Object kinetic Monte Carlo simulation of tungsten cascade aging. *J. Nucl. Mater.* 462, 338–344. doi:10.1016/j.jnucmat.2014.09.067.
134. Nandipati, G., Setyawan, W., Heinisch, H.L., *et al.*, 2015. Displacement cascades and defect annealing in tungsten, Part III: The sensitivity of cascade annealing in tungsten to the values of kinetic parameters. *J. Nucl. Mater.* 462, 345–353. doi:10.1016/j.jnucmat.2015.01.059.
135. Miller, M.K., Stoller, R.E., Russell, K.F., 1996. Effect of neutron-irradiation on the spinodal decomposition of Fe-32% Cr model alloy. *J. Nucl. Mater.* 230, 219–225. doi:10.1016/0022-3115(96)80017-1.
136. Hornbogen, E., Glenn, R.C., 1960. A metallographic study of precipitation of copper from alpha iron. *Trans. Met. Soc. AIME* 218, 1064.
137. Khrushcheva, O., Zhurkin, E.E., Malerba, L., *et al.*, 2003. Copper precipitation in iron: A comparison between metropolis Monte Carlo and lattice kinetic Monte Carlo methods. *Nucl. Instrum. Methods Phys. Res. Sect. B Beam Interact. Mater. At.* 202, 68–75. doi:10.1016/S0168-583X(02)01830-X.
138. Monasterio, P.R., Wirth, B.D., Odette, G.R., 2007. Kinetic Monte Carlo modeling of cascade aging and damage accumulation in Fe–Cu alloys. *J. Nucl. Mater.* 361, 127–140. doi:10.1016/j.jnucmat.2006.12.022.
139. Pascuet, M.I., Castin, N., Becquart, C.S., Malerba, L., 2011. Stability and mobility of Cu–vacancy clusters in Fe–Cu alloys: A computational study based on the use of artificial neural networks for energy barrier calculations. *J. Nucl. Mater.* 412, 106–115. doi:10.1016/j.jnucmat.2011.02.038.
140. Schmauder, S., Binkele, P., 2002. Atomistic computer simulation of the formation of Cu-precipitates in steels. *Comput. Mater. Sci.* 24, 42–53. doi:10.1016/S0927-0256(02)00163-5.
141. Wirth, B.D., Odette, G.R., 1998. Kinetic Lattice Monte Carlo simulations of diffusion and decomposition kinetics in Fe-Cu alloys: Embedded atom and nearest neighbor potentials. *Mater. Res. Soc. Symp. Proc.* 151–155.

142. Castin, N., Malerba, L., Bonny, G., *et al.*, 2009. Modelling radiation-induced phase changes in binary FeCu and ternary FeCuNi alloys using an artificial intelligence-based atomistic kinetic Monte Carlo approach. *Nucl. Instrum. Methods Phys. Res. Sect. B Beam Interact. Mater. At.* 267, 3002–3008. doi:10.1016/j.nimb.2009.06.092.
143. Djurabekova, F.G., Domingos, R., Cerchiara, G., *et al.*, 2007. Artificial intelligence applied to atomistic kinetic Monte Carlo simulations in Fe–Cu alloys. *Nucl. Instrum. Methods Phys. Res. Sect. B Beam Interact. Mater. At.* 255, 8–12. doi:10.1016/j.nimb.2006.11.039.
144. Domain, C., Becquart, C.S., Van, D., 1999. Kinetic Monte Carlo simulations of FeCu alloys. *Mater. Res. Soc. Symp. Proc.* 538, 217–222.
145. Soisson, F., Becquart, C.S., Castin, N., *et al.*, 2010. Atomistic Kinetic Monte Carlo studies of microchemical evolutions driven by diffusion processes under irradiation. *J. Nucl. Mater.* 406, 55–67. doi:10.1016/j.jnucmat.2010.05.018.
146. Vincent, E., Becquart, C.S., Domain, C., 2006. Solute interaction with point defects in a Fe during thermal ageing: A combined ab initio and atomic kinetic Monte Carlo approach. *J. Nucl. Mater.* 351, 88–99. doi:10.1016/j.jnucmat.2006.02.018.
147. Bonny, G., Pasianot, R.C., Castin, N., Malerba, L., 2009. Ternary Fe–Cu–Ni many-body potential to model reactor pressure vessel steels: First validation by simulated thermal annealing. *Philos. Mag.* 89, 3531–3546. doi:10.1080/14786430903299824.
148. Wang, Y., Yin, J., Liu, X., *et al.*, 2017. Precipitation kinetics in binary Fe–Cu and ternary Fe–Cu–Ni alloys via kMC method. *Prog. Nat. Sci. Mater. Int.* 27, 460–466. doi:10.1016/j.pnsc.2017.06.005.
149. Soisson, F., Fu, C.-C., 2007. Cu-precipitation kinetics in a-Fe from atomistic simulations: Vacancy-trapping effects and Cu-cluster mobility. *Phys. Rev. B* 76, 214102. doi:10.1103/PhysRevB.76.214102.
150. Ngayam-Happy, R., Becquart, C.S., Domain, C., Malerba, L., 2012. Formation and evolution of MnNi clusters in neutron irradiated dilute Fe alloys modelled by a first principle-based AKMC method. *J. Nucl. Mater.* 426, 198–207. doi:10.1016/j.jnucmat.2012.03.033.
151. Bonny, G., Terentyev, D., Bakaev, A., *et al.*, 2013. On the thermal stability of late blooming phases in reactor pressure vessel steels: An atomistic study. *J. Nucl. Mater.* 442, 282–291. doi:10.1016/j.jnucmat.2013.08.018.
152. Odette, G.R., Nansstad, R.K., 2009. Predictive reactor pressure vessel steel irradiation embrittlement models: Issues and opportunities. *JOM* 61, 17–23. doi:10.1007/s11837-009-0097-4.
153. Pareige, C., Domain, C., Olsson, P., 2009. Short- and long-range orders in Fe–Cr: A Monte Carlo study. *J. Appl. Phys.* 106, 104906. doi:10.1063/1.3257232.
154. Pareige, C., Roussel, M., Novy, S., *et al.*, 2011. Kinetic study of phase transformation in a highly concentrated Fe–Cr alloy: Monte Carlo simulation versus experiments. *Acta Mater.* 59, 2404–2411. doi:10.1016/j.actamat.2010.12.038.
155. Soisson, F., Jourdan, T., 2016. Radiation-accelerated precipitation in Fe–Cr alloys. *Acta Mater.* 103, 870–881. doi:10.1016/j.actamat.2015.11.001.
156. Wallenius, J., Olsson, P., Malerba, L., Terentyev, D., 2007. Simulation of thermal ageing and radiation damage in Fe–Cr. *Nucl. Instrum. Methods Phys. Res. Sect. B Beam Interact. Mater. At.* 255, 68–74. doi:10.1016/j.nimb.2006.11.063.
157. Senninger, O., Soisson, F., Martínez, E., *et al.*, 2016. Modeling radiation induced segregation in iron–chromium alloys. *Acta Mater.* 103, 1–11. doi:10.1016/j.actamat.2015.09.058.
158. Heinisch, H.L., Weber, W.J., 2005. Computational model of alpha-decay damage accumulation in zircon. *Nucl. Instrum. Methods Phys. Res. Sect. B Beam Interact. Mater. At.* 228, 293–298. doi:10.1016/j.nimb.2004.10.059.
159. Ejenstam, J., Thuvander, M., Olsson, P., *et al.*, 2015. Microstructural stability of Fe–Cr–Al alloys at 450–550°C. *J. Nucl. Mater.* 457, 291–297. doi:10.1016/j.jnucmat.2014.11.101.
160. Zhang, X., Shu, S., Bellon, P., Averback, R.S., 2015. Precipitate stability in Cu–Ag–W system under high-temperature irradiation. *Acta Mater.* 97, 348–356. doi:10.1016/j.actamat.2015.06.045.
161. Zhang, X., Beach, J.A., Wang, M., *et al.*, 2016. Precipitation kinetics of dilute Cu–W alloys during low-temperature ion irradiation. *Acta Mater.* 120, 46–55. doi:10.1016/j.actamat.2016.08.043.
162. Vu, T.H.Y., Ramjaun, Y., Hayoun, M., *et al.*, 2015. On the evolution of the steady state in gold-silica nanocomposites under sustained irradiation. *J. Appl. Phys.* 117, 174305. doi:10.1063/1.4919019.
163. Becquart, C.S., Mousseau, N., Domain, C., 2018. *Atomistic Kinetic Monte Carlo and Solute Effects*. Andreoni, W., Yip, S. (Eds.), Singapore: Springer International Publishing AG, Part of Springer Nature.
164. Hobler, G., Otto, G., 2003. Status and open problems in modeling of as-implanted damage in silicon. *Mater. Sci. Semicond. Process.* 6, 1–14. doi:10.1016/S1369-8001(03)00065-9.
165. Castin, N., Bonny, G., Bakaev, A., *et al.*, 2018. Object kinetic Monte Carlo model for neutron and ion irradiation in tungsten: Impact of transmutation and carbon impurities. *J. Nucl. Mater.* 500, 15–25. doi:10.1016/j.jnucmat.2017.12.014.
166. Fluss, M.J., Wirth, B.D., Wall, M., *et al.*, 2004. Temperature-dependent defect properties from ion-irradiation in Pu(Ga). *J. Alloy. Compd.* 368, 62–74. doi:10.1016/j.jallcom.2003.08.080.
167. Perlado, J.M., Lodi, D., Marian, J., *et al.*, 2003. Time-dependent neutronics in structural materials of inertial fusion reactors and simulation of defect accumulation in pulsed Fe and SiC. *Fusion Sci. Technol.* 43, 384–392. doi:10.13182/FST03-A282.
168. Soneda, N., Ishino, S., Takahashi, A., Dohi, K., 2003. Modeling the microstructural evolution in bcc-Fe during irradiation using kinetic Monte Carlo computer simulation. *J. Nucl. Mater.* 323, 169–180. doi:10.1016/j.jnucmat.2003.08.021.
169. Choi, Y.H., Joo, H.G., 2013. Multiscale simulation of neutron induced damage in tritium breeding blankets with different spectral shifters. *Fusion Eng. Des.* 88, 2471–2475. doi:10.1016/j.fusengdes.2013.05.085.
170. Chiapetto, M., Becquart, C.S., Malerba, L., 2016. Simulation of nanostructural evolution under irradiation in Fe-9%Cr alloys: An object kinetic Monte Carlo study of the effect of temperature and dose-rate. *Nucl. Mater. Energy* 9, 565–570. doi:10.1016/j.nme.2016.04.009.
171. Arévalo, C., Caturla, M.J., Perlado, J.M., 2007. Temperature dependence of damage accumulation in  $\alpha$ -zirconium. *J. Nucl. Mater.* 367–370, 338–343. doi:10.1016/j.jnucmat.2007.03.131.
172. Gámez, L., Martínez, E., Perlado, J.M., *et al.*, 2007. Kinetic Monte Carlo modelling of neutron irradiation damage in iron. *Fusion Eng. Des.* 82, 2666–2670. doi:10.1016/j.fusengdes.2007.04.040.
173. Caturla, M.-J., Wall, M., Alonso, E., *et al.*, 2000. Heavy ion irradiation and annealing of lead: Atomistic simulations and experimental validation. *J. Nucl. Mater.* 276, 186–193. doi:10.1016/S0022-3115(99)00202-0.
174. Caturla, M.J., Soneda, N., Alonso, E., *et al.*, 2000. Comparative study of radiation damage accumulation in Cu and Fe. *J. Nucl. Mater.* 276, 13–21. doi:10.1016/S0022-3115(99)00220-2.
175. Marian, J., Wirth, B.D., Perlado, J.M., *et al.*, 2001. Direct comparison between modeling and experiment: An a-Fe ion implantation study. *Mater. Res. Soc. Symp. Proc.* R3.2.1–R3.2.6.
176. Perlado, J.M., Malerba, L., de la, R., 1998. MD simulation of high energy cascades and damage accumulation in  $\beta$ -SiC in inertial fusion conditions. *Fusion Technol.* 34, 840–847.
177. Warriar, M., Bhardwaj, U., Bukkuru, S., 2016. Multi-scale modeling of radiation damage: Large scale data analysis. *J. Phys. Conf. Ser.* 759, 012078. doi:10.1088/1742-6596/759/1/012078.
178. Wirth, B.D., Caturla, M.J., Diaz de la Rubia, T., *et al.*, 2001. Mechanical property degradation in irradiated materials: A multiscale modeling approach. *Nucl. Instrum. Methods Phys. Res. Sect. B Beam Interact. Mater. At.* 180, 23–31. doi:10.1016/S0168-583X(01)00392-5.
179. Otto, G., Kovac, D., Hobler, G., 2005. Coupled BC/KLMC simulations of the temperature dependence of implant damage formation in silicon. *Nucl. Instrum. Methods Phys. Res. Sect. B Beam Interact. Mater. At.* 228, 256–259. doi:10.1016/j.nimb.2004.10.054.
180. Payet, A., Luce, F.P., Curfs, C., *et al.*, 2016. Damage accumulation during cryogenic and room temperature implantations in strained SiGe alloys. *Mater. Sci. Semicond. Process.* 42, 247–250. doi:10.1016/j.mssp.2015.07.059.

181. Hobler, G., Otto, G., Kovac, D., *et al.*, 2005. Multiscale approach for the analysis of channeling profile measurements of ion implantation damage. *Nucl. Instrum. Methods Phys. Res. Sect. B Beam Interact. Mater. At.* 228, 360–363. doi:10.1016/j.nimb.2004.10.070.
182. Caturla, M.J., Diaz de la Rubia, T., Victoria, M., *et al.*, 2001. Multiscale modeling of radiation damage: Applications to damage production by GeV proton irradiation of Cu and W, and pulsed irradiation effects in Cu and Fe. *J. Nucl. Mater.* 296, 90–100. doi:10.1016/S0022-3115(01)00569-4.
183. Hehr, B.D., 2014. Analysis of radiation effects in silicon using kinetic monte carlo methods. *IEEE Trans. Nucl. Sci.* 61, 2847–2854. doi:10.1109/TNS.2014.2368075.
184. Ito, A.M., Kato, S., Takayama, A., Nakamura, H., 2017. Automatic kinetic Monte-Carlo modeling for impurity atom diffusion in grain boundary structure of tungsten material. *Nucl. Mater. Energy* 12, 353–360. doi:10.1016/j.nme.2017.04.010.
185. Ramasubramaniam, A., Itakura, M., Ortiz, M., Carter, E.A., 2008. Effect of atomic scale plasticity on hydrogen diffusion in iron: Quantum mechanically informed and on-the-fly kinetic Monte Carlo simulations. *J. Mater. Res.* 23, 2757–2773. doi:10.1557/JMR.2008.0340.
186. Yang, X., Oyeniyi, W.O., 2017. Kinetic Monte Carlo simulation of hydrogen diffusion in tungsten. *Fusion Eng. Des.* 114, 113–117. doi:10.1016/j.fusengdes.2016.12.012.
187. Oda, T., Tanaka, S., 2011. Modeling of diffusivity of tritium interacting with F centers in Li<sub>2</sub>O. *J. Nucl. Mater.* 417, 743–747. doi:10.1016/j.jnucmat.2010.12.132.
188. Yang, X., Hassanein, A., 2014. Kinetic Monte Carlo simulation of hydrogen diffusion on tungsten reconstructed (001) surface. *Fusion Eng. Des.* 89, 2545–2549. doi:10.1016/j.fusengdes.2014.06.001.
189. Dai, Y., 2020. *The Effects of Helium in Irradiated Structural Alloys*, *Comprehensive Nuclear Materials*, second ed, vol. 1. Elsevier, pp. 186–234.
190. Martínez, E., Schwen, D., Caro, A., 2015. Helium segregation to screw and edge dislocations in  $\alpha$ -iron and their yield strength. *Acta Mater.* 84, 208–214. doi:10.1016/j.actamat.2014.10.066.
191. Erhart, P., Marian, J., 2011. Calculation of the substitutional fraction of ion-implanted He in an  $\alpha$ -Fe target. *J. Nucl. Mater.* 414, 426–430. doi:10.1016/j.jnucmat.2011.05.017.
192. Yang, Z., Blondel, S., Hammond, K.D., Wirth, B.D., 2017. Kinetic Monte Carlo simulations of helium cluster nucleation in tungsten with preexisting vacancies. *Fusion Sci. Technol.* 71, 60–74. doi:10.13182/FST16-111.
193. Sharafat, S., Takahashi, A., Nagasawa, K., Ghoniem, N., 2009. A description of stress driven bubble growth of helium implanted tungsten. *J. Nucl. Mater.* 389, 203–212. doi:10.1016/j.jnucmat.2009.02.027.
194. Rivera, A., Valles, G., Caturla, M.J., Martín-Bragado, I., 2013. Effect of ion flux on helium retention in helium-irradiated tungsten. *Nucl. Instrum. Methods Phys. Res. Sect. B Beam Interact. Mater. At.* 303, 81–83. doi:10.1016/j.nimb.2012.10.038.
195. Morishita, K., Sugano, R., Wirth, B.D., 2003. Thermal stability of helium-vacancy clusters and bubble formation – Multiscale modeling approach for fusion materials development. *Fusion Sci. Technol.* 44, 441–445. doi:10.13182/FST03-A374.
196. Perez, D., Sandoval, L., Blondel, S., *et al.*, 2017. The mobility of small vacancy/helium complexes in tungsten and its impact on retention in fusion-relevant conditions. *Sci. Rep.* 7, 2522. doi:10.1038/s41598-017-02428-2.
197. Wirth, B.D., Bringa, E.M., 2004. A kinetic monte carlo model for helium diffusion and clustering in fusion environments. *Phys. Scr.* 80–84.
198. Bringa, E.M., Wirth, B.D., Caturla, M.J., *et al.*, 2003. Metals far from equilibrium: From shocks to radiation damage. *Nucl. Instrum. Methods Phys. Res. Sect. B Beam Interact. Mater. At.* 202, 56–63. doi:10.1016/S0168-583X(02)01831-1.
199. Caturla, M.J., Diaz de la Rubia, T., Fluss, M., 2003. Modeling microstructure evolution of f.c.c. metals under irradiation in the presence of He. *J. Nucl. Mater.* 323, 163–168. doi:10.1016/j.jnucmat.2003.08.003.
200. De Backer, A., Adjanor, G., Domain, C., *et al.*, 2015. Modeling of helium bubble nucleation and growth in austenitic stainless steels using an Object Kinetic Monte Carlo method. *Nucl. Instrum. Methods Phys. Res. Sect. B Beam Interact. Mater. At.* 352, 107–114. doi:10.1016/j.nimb.2014.11.110.
201. Deo, C.S., Okuniewski, M.A., Srivilliputhur, S.G., *et al.*, 2007. Helium bubble nucleation in bcc iron studied by kinetic Monte Carlo simulations. *J. Nucl. Mater.* 361, 141–148. doi:10.1016/j.jnucmat.2006.12.018.
202. Guo, X., Zhang, X., Xue, J., Li, W., 2013. KMC simulation of helium bubble formation in  $\alpha$ -Fe. *Nucl. Instrum. Methods Phys. Res. Sect. B Beam Interact. Mater. At.* 307, 77–80. doi:10.1016/j.nimb.2012.12.108.
203. De Backer, A., Ortiz, C.J., Domain, C., *et al.*, 2013. Spatial effects in the 800 keV 3He implantation in W followed by isochronal annealing at 900 K. *Nucl. Instrum. Methods Phys. Res. Sect. B Beam Interact. Mater. At.* 303, 87–90. doi:10.1016/j.nimb.2012.10.025.
204. Galloway, G.J., Ackland, G.J., 2013. Molecular dynamics and object kinetic Monte Carlo study of radiation-induced motion of voids and He bubbles in bcc iron. *Phys. Rev. B* 87, 104106. doi:10.1103/PhysRevB.87.104106.
205. Gámez, B., Gámez, L., Ortiz, C.J., *et al.*, 2009. Object Kinetic Monte Carlo calculations of electron and He irradiation of nickel. *J. Nucl. Mater.* 386–388, 90–92. doi:10.1016/j.jnucmat.2008.12.066.
206. Suzudo, T., Yamaguchi, M., Kabraki, H., Ebihara, K.I., 2010. Multiscale modeling of helium-vacancy cluster nucleation under irradiation: A kinetic Monte-Carlo approach. *Mater. Res. Soc. Symp. Proc.* 29–35.
207. Valles, G., Martín-Bragado, I., Nordlund, K., *et al.*, 2017. Temperature dependence of underdense nanostructure formation in tungsten under helium irradiation. *J. Nucl. Mater.* 490, 108–114. doi:10.1016/j.jnucmat.2017.04.021.
208. Maillard, S., Martin, G., Sabathier, C., 2016. Why a steady state void size distribution in irradiated UO<sub>2</sub>? A modeling approach. *Nucl. Instrum. Methods Phys. Res. Sect. B Beam Interact. Mater. At.* 374, 58–66. doi:10.1016/j.nimb.2015.09.068.
209. Oaks, A., Yun, D., Ye, B., *et al.*, 2011. Kinetic Monte Carlo model of defect transport and irradiation effects in La-doped CeO<sub>2</sub>. *J. Nucl. Mater.* 414, 145–149. doi:10.1016/j.jnucmat.2011.02.030.
210. Behera, R.K., Watanabe, T., Andersson, D.A., *et al.*, 2016. Diffusion of oxygen interstitials in UO<sub>2+x</sub> using kinetic Monte Carlo simulations: Role of O/M ratio and sensitivity analysis. *J. Nucl. Mater.* 472, 89–98. doi:10.1016/j.jnucmat.2016.02.003.
211. Bertolus, M., Freyss, M., Dorado, B., *et al.*, 2015. Linking atomic and mesoscopic scales for the modelling of the transport properties of uranium dioxide under irradiation. *J. Nucl. Mater.* 462, 475–495. doi:10.1016/j.jnucmat.2015.02.026.
212. Méric de Bellefon, G., Wirth, B.D., 2011. Kinetic Monte Carlo (KMC) simulation of fission product silver transport through TRISO fuel particle. *J. Nucl. Mater.* 413, 122–131. doi:10.1016/j.jnucmat.2011.04.010.
213. Al Toooq, Z., Kenny, S.D., 2013. Modelling radiation damage at grain boundaries in fcc Nickel and Ni-based alloy using Long Time Scale Dynamics Techniques. *Nucl. Instrum. Methods Phys. Res. Sect. B Beam Interact. Mater. At.* 303, 9–13. doi:10.1016/j.nimb.2012.10.027.
214. Li, X., Liu, W., Xu, Y., *et al.*, 2016. Radiation resistance of nano-crystalline iron: Coupling of the fundamental segregation process and the annihilation of interstitials and vacancies near the grain boundaries. *Acta Mater.* 109, 115–127. doi:10.1016/j.actamat.2016.02.028.
215. Valles, G., Panizo-Laiz, M., González, C., *et al.*, 2017. Influence of grain boundaries on the radiation-induced defects and hydrogen in nanostructured and coarse-grained tungsten. *Acta Mater.* 122, 277–286. doi:10.1016/j.actamat.2016.10.007.
216. Pedersen, A., Jónsson, H., 2009. Simulations of hydrogen diffusion at grain boundaries in aluminum. *Acta Mater.* 57, 4036–4045. doi:10.1016/j.actamat.2009.04.057.
217. Uberuaga, B.P., Andersson, D.A., 2015. Uranium vacancy mobility at the S5 symmetric tilt and S5 twist grain boundaries in UO<sub>2</sub>. *Comput. Mater. Sci.* 108, 80–87. doi:10.1016/j.commatsci.2015.06.017.
218. Ko, H., Deng, J., Szlufarska, I., Morgan, D., 2016. Ag diffusion in SiC high-energy grain boundaries: Kinetic Monte Carlo study with first-principle calculations. *Comput. Mater. Sci.* 121, 248–257. doi:10.1016/j.commatsci.2016.04.027.
219. Ko, H., Szlufarska, I., Morgan, D., 2017. Cs diffusion in SiC high-energy grain boundaries. *J. Appl. Phys.* 122, 105901. doi:10.1063/1.4989389.
220. Oudriss, A., Creus, J., Bouhattate, J., *et al.*, 2012. Grain size and grain-boundary effects on diffusion and trapping of hydrogen in pure nickel. *Acta Mater.* 60, 6814–6828. doi:10.1016/j.actamat.2012.09.004.

221. Chiapetto, M., Malerba, L., Puype, A., Becquart, C.S., 2016. Object kinetic Monte Carlo study of the effect of grain boundaries in martensitic Fe–Cr–C alloys. *Phys. Status Solidi A* 213, 2981–2987. doi:10.1002/pssa.201600294.
222. Golubov, S., 2020. Mean Field Rate Theory of Radiation Damage, *Comprehensive Nuclear Materials, second ed, vol. 1*. Elsevier, pp. 717–753.
223. Ahlgren, T., Bukonte, L., 2017. Sink strength simulations using the Monte Carlo method: Applied to spherical traps. *J. Nucl. Mater.* 496, 66–76. doi:10.1016/j.jnucmat.2017.09.006.
224. Malerba, L., Becquart, C.S., Domain, C., 2007. Object kinetic Monte Carlo study of sink strengths. *J. Nucl. Mater.* 360, 159–169. doi:10.1016/j.jnucmat.2006.10.002.
225. Martínez, E., Senninger, O., Caro, A., *et al.*, 2018. Role of sink density in nonequilibrium chemical redistribution in alloys. *Phys. Rev. Lett.* 120, 106101. doi:10.1103/PhysRevLett.120.106101.
226. Sivak, A.B., Sivak, P.A., Romanov, V.A., Chernov, V.M., 2015. Effect of external stresses on efficiency of dislocation sinks in BCC (Fe, V) and FCC (Cu) crystals. *Inorg. Mater. Appl. Res.* 6, 466–472. doi:10.1134/S2075113315050184.
227. Vattré, A., Jourdan, T., Ding, H., *et al.*, 2016. Non-random walk diffusion enhances the sink strength of semicoherent interfaces. *Nat. Commun.* 7, 10424. doi:10.1038/ncomms10424.
228. Carpentier, D., Jourdan, T., Le Bouar, Y., Marinica, M.-C., 2017. Effect of saddle point anisotropy of point defects on their absorption by dislocations and cavities. *Acta Mater.* 136, 323–334. doi:10.1016/j.actamat.2017.07.013.
229. Heinisch, H.L., Trinkaus, H., Singh, B.N., 2007. Kinetic Monte Carlo studies of the reaction kinetics of crystal defects that diffuse one-dimensionally with occasional transverse migration. *J. Nucl. Mater.* 367–370, 332–337. doi:10.1016/j.jnucmat.2007.03.034.
230. Hou, J., Kong, X.-S., Li, X.-Y., *et al.*, 2016. Modification on theory of sink strength: An Object Kinetic Monte Carlo study. *Comput. Mater. Sci.* 123, 148–157. doi:10.1016/j.commatsci.2016.06.024.
231. Stoller, R.E., Golubov, S.I., Domain, C., Becquart, C.S., 2008. Mean field rate theory and object kinetic Monte Carlo: A comparison of kinetic models. *J. Nucl. Mater.* 382, 77–90. doi:10.1016/j.jnucmat.2008.08.047.
232. Rottler, J., Srolovitz, D.J., Car, R., 2007. Kinetic Monte Carlo study of radiation-induced segregation in model metallic alloys. *Philos. Mag.* 87, 3945–3958. doi:10.1080/14786430701429904.
233. Xu, D., Wirth, B.D., Li, M., Kirk, M.A., 2012. Defect microstructural evolution in ion irradiated metallic nanofolios: Kinetic Monte Carlo simulation versus cluster dynamics modeling and in situ transmission electron microscopy experiments. *Appl. Phys. Lett.* 101, 101905. doi:10.1063/1.4748980.
234. Becquart, C.S., Domain, C., 2011. Modeling microstructure and irradiation effects. *Metall. Mater. Trans. Phys. Metall. Mater. Sci.* 42, 852–870. doi:10.1007/s11661-010-0460-7.
235. Jumel, S., Domain, C., Ruste, J., *et al.*, 2002. Simulation of irradiation effects in reactor pressure vessel steels: The reactor for virtual experiments (REVE) project. *J. Test. Eval.* 30, 37–46.
236. Castin, N., Pascuet, M.I., Malerba, L., 2011. Modeling the first stages of Cu precipitation in a-Fe using a hybrid atomistic kinetic Monte Carlo approach. *J. Chem. Phys.* 135, 064502. doi:10.1063/1.3622045.
237. Pannier, B., 2017. Towards the Prediction of Microstructure Evolution Under Irradiation of Model Ferritic Alloys With an Hybrid AKMC-OKMC Approach (PhD Dissertation). Université Lille.
238. Becquart, C.S., Domain, C., Legris, A., Van Duysen, J.C., 2000. Influence of the interatomic potentials on molecular dynamics simulations of displacement cascades. *J. Nucl. Mater.* 280, 73–85. doi:10.1016/S0022-3115(00)00029-5.
239. Aliaga, M.J., Dopico, I., Martín-Bragado, I., Caturia, M.J., 2016. Influence of free surfaces on microstructure evolution of radiation damage in Fe from molecular dynamics and object kinetic Monte Carlo calculations: Influence of free surfaces on microstructure evolution of radiation damage in Fe. *Phys. Status Solidi A* 213, 2969–2973. doi:10.1002/pssa.201600158.
240. Duan, G., Li, X., Xu, Y., *et al.*, 2018. Clustering and segregation of small vacancy clusters near tungsten (001) surface. *Nucl. Instrum. Methods Phys. Res. Sect. B Beam Interact. Mater. At.* 414, 29–37. doi:10.1016/j.nimb.2017.10.007.
241. Hoffman, R.T., Moore, A.P., Deo, C.S., 2016. Examination of the effect of vacancy detachment rates on kinetic Monte Carlo simulations of bcc metals. *MRS Adv.* 1, 2489–2494. doi:10.1557/adv.2016.513.
242. Wu, B., Li, S., Zhang, Y., 2015. Optimizing parallel kinetic Monte Carlo simulation by communication aggregation and scheduling. In: *Big Data Technology and Applications*. Singapore: Springer, pp. 282–297.
243. Martínez, E., Marian, J., Kalos, M.H., Perlado, J.M., 2008. Synchronous parallel kinetic Monte Carlo for continuum diffusion-reaction systems. *J. Comput. Phys.* 227, 3804–3823. doi:10.1016/j.jcp.2007.11.045.
244. Martín-Bragado, I., Abujas, J., Galindo, P.L., Pizarro, J., 2015. Synchronous parallel Kinetic Monte Carlo: Implementation and results for object and lattice approaches. *Nucl. Instrum. Methods Phys. Res. Sect. B Beam Interact. Mater. At.* 352, 27–30. doi:10.1016/j.nimb.2014.12.081.
245. Jiménez, F., Ortiz, C.J., 2016. A GPU-based parallel Object kinetic Monte Carlo algorithm for the evolution of defects in irradiated materials. *Comput. Mater. Sci.* 113, 178–186. doi:10.1016/j.commatsci.2015.11.011.
246. Donev, A., Bulatov, V.V., Opperstrup, T., *et al.*, 2010. A first-passage kinetic Monte Carlo algorithm for complex diffusion–reaction systems. *J. Comput. Phys.* 229, 3214–3236. doi:10.1016/j.jcp.2009.12.038.
247. Athènes, M., Bulatov, V.V., 2014. Path factorization approach to stochastic simulations. *Phys. Rev. Lett.* 113. doi:10.1103/PhysRevLett.113.230601.
248. Danielson, T., Sutton, J.E., Hin, C., Savara, A., 2017. SQERTSS: Dynamic rank based throttling of transition probabilities in kinetic Monte Carlo simulations. *Comput. Phys. Commun.* 219, 149–163. doi:10.1016/j.cpc.2017.05.016.
249. Messina, L., Castin, N., Domain, C., Olsson, P., 2017. Introducing *ab initio* based neural networks for transition-rate prediction in kinetic Monte Carlo simulations. *Phys. Rev. B* 95. doi:10.1103/PhysRevB.95.064112.
250. Behler, J., 2016. Perspective: Machine learning potentials for atomistic simulations. *J. Chem. Phys.* 145, 170901. doi:10.1063/1.4966192.
251. Brommer, P., Kiselev, A., Schopf, D., *et al.*, 2015. Classical interaction potentials for diverse materials from *ab initio* data: A review of potfit. *Model. Simul. Mater. Sci. Eng.* 23, 074002. doi:10.1088/0965-0393/23/7/074002.